博士論文

Studies on the structure and function of fatty acid desaturase

（脂肪酸不飽和化酵素の構造と機能に関する研究）

渡邉　研志

広島大学大学院先端物質科学研究科

2016 年 3 月

目次

1．主論文

Studies on the structure and function of fatty acid desaturase

(脂肪酸不飽和化酵素の構造と機能に関する研究)

渡邉　研志

2．公表論文

（1）Identification of amino acid residues that determine the substrate specificity of mammalian membrane-bound front-end fatty acid desaturases

K. Watanabe, M. Ohno, M. Taguchi, S. Kawamoto, K. Ono, T. Aki

Journal of Lipid Research, **57**, 89-99 (2016)

（2）Detection of acyl-CoA derivatized with butylamide for *in vitro* fatty acid desaturase assay

K. Watanabe, M. Ohno, T. Aki

Journal of Oleo Science, **65**, 161-167 (2016)

主論文

Contents

1. Preface

Fatty acids are carbonic acids that have long and straight alkyl chain, and they play essential roles on energy storage and conformation of hydrophobic region of biological membrane. Biosynthesis of fatty acid is performed by fatty acid synthase (1), and palmitic acid (16:0) with 16 carbons is synthesized in the beginning. Palmitic acid is converted to stearic acid (18:0), and various fatty acids are produced by a variety of fatty acid-modifying systems of each species (Fig. 1).

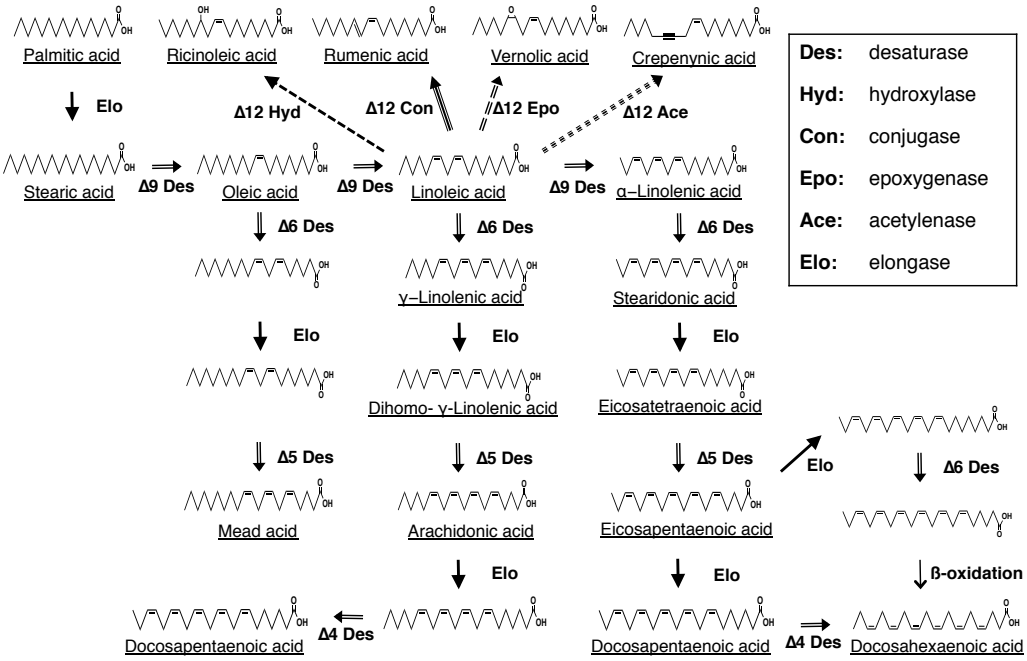

Figure 1. Fatty acid modifying of eukaryotes catalyzed by desaturase family enzymes.

Unsaturated fatty acids synthesized by introduction of double bonds into carbon hydrate chain by catalyzed by fatty acid desaturases maintain the fluidity of biological membrane. Especially, fatty acids which contain more than 4 double bonds such as arachidonic acid (ARA; 20:4 Δ5,8,11,14), eicosapentaenoic acid (EPA; 20:5 Δ5,8,11,14,17) and docosahexaenoic acid (DHA; 22:6 Δ4,7,10,13,16,19) are called polyunsaturated fatty acid (PUFA) (2). These fatty acids are reported to be essential for development of infant brain or maintaining of eye function (3–5). Moreover, PUFAs are converted to biologically active

substance such as eicosanoids (6) that have improving action on inflammatory disease or diabetes (7) and, they are used for pharmaceuticals and health food. Hydroxyl fatty acid, which is produced by fatty acid hydroxylase, is component of wax esters of plant surface and exerts protective functions against environmental stress (8). Acetylenic fatty acids are anti-fungal reagent in plant (9). Epoxydized fatty acids contained in the plant seeds are mediators involved in inflammatory responses or regulation of blood pressure (10). Conjugated fatty acids are contained in meat of ruminants, and various health promotion effects including carcinogenesis suppressing function or regulation of immune function, are reported (11). Like these fatty acids, the structures and functions of fatty acids are diversified by fatty acid modifying-enzymes of each species.

These enzymes which constitute the fatty acid modifying-systems are called desaturase family, and they are classified into water soluble type enzymes which act on fatty acid bound to acyl carrier protein (ACP) (12) and membrane-bound type enzymes which use fatty acids bound to coenzyme A (13, 14) or lysophosphatidic acid as substrate (15, 16). Among them, membrane-bound desaturases are responsible for various modification reactions described above. Membrane-bound enzymes of this family bind to biological membrane with two large hydrophobic regions that separate three hydrophilic domains. There are three histidine clusters which form the catalytic center by coordinating non-heme di-iron (17) in hydrophilic domains (Fig. 2). Although these common structure suggest that the three dimensional structures of these enzymes are presumed to be similar, there are a variety of enzymes with various substrate specificities and regioselectivities as shown in Fig. 1. Comparing the number of previous reports, the reports about membrane-bound enzymes overwhelmingly exceed those of water soluble type enzymes. However, in contrast to water soluble type enzymes of which crystal structures were elucidated earlier (18), the knowledge about the structure of membrane-bound enzymes are prevented by the difficulty of purification. Although some domains and amino acids are presumed to concern the recognition of substrate in several enzymes (19–21), the exact

molecular mechanisms that define the various reaction specificities are unclear. The crystal structure of Δ9 stearoyl-CoA desaturase (SCD1) of human, which is the membrane-bound type enzyme, was elucidated recently (22, 23), and the part of substrate-recognition mechanism was revealed. However, the information of structure-function relationship of membrane-bound enzymes is still limited compared to that of soluble enzymes.

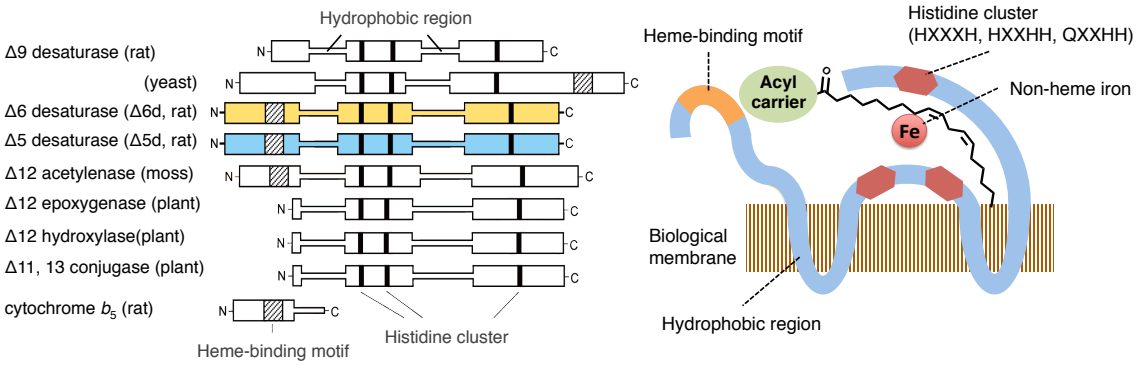

Figure 2. Predicted membrane topology of desaturase family.

The information about the molecular mechanism which determines the function of each enzyme is important for drag designs targeting the certain protein involved in a particular disease (24, 25) or efficient production of enzymes with desired functions. In the case of fatty acid modifying enzymes, the knowledge of structure-function relationship permits the production of enzymes that can perform the specific modifications to any portion of the hydrocarbon chains. Such enzymes are expected to be applied to the design of high value-added fatty acids such as rare fatty acids or novel fatty acids with new physiological activities. Specific structured lipids of which functions including the melting point or absorbability are produced by artificially alteration of fatty acid composition are used in food and medicine field (26). By combining this technic with designed fatty acid, the applicability of functional lipids spread infinitely.

In my thesis, I aimed to get the knowledge about structure-function relationship of membrane-bound fatty acid modifying enzymes that are responsible for the production of high

value-added fatty acids. I chose Δ6 and Δ5 fatty acid desaturases (D6d and D5d) from *Rattus norvegicus* (13, 27) as research model enzymes. They have common domains of membrane-bound desaturase family enzymes described above, and play the main roles on the synthesis of PUFAs. Although their primary structures are highly homologous, they express mutually exclusive substrate specificities (Fig. 1). Thus these enzymes were conceived suitable model for elucidation of structure-function relationship of desaturase family enzymes that express various reaction specificities despite of similar structures. Chapter 2 consists of the identification of amino acids that determine the substrate specificities of D6d and D5d. Chapter 3 contains the measuring the activity of acyl-CoA desaturases with a simplified *in vitro* reaction method. Chapter 4 consists of purification of D6d and D5d. Chapter 5 is the general conclusion of this thesis.

In chapter 2, I examined the amino acids that define the substrate specificities of D6d and D5d. Since amino acid sequences of D6d and D5d from *R. norvegicus* are highly homologous, these enzymes are inferred to have very similar three-dimensional structures. Therefore, it is considered that the difference in substrate specificity between these enzymes can be attributed to particular amino acids. A functional analysis of chimeric enzymes produced by domain-swapping and site-directed mutagenesis showed that some amino acids that are responsible for recognition of substrate. Furthermore, homology modeling on the basis of the crystal structure of human SCD1 revealed the mechanism of substrate recognition by those amino acids.

In chapter 3, I proposed the simplified method to measure the activity of acyl-CoA desaturases. Desaturases of higher animals including D6d and D5d act on fatty acids bound to CoA, and variety of enzymes that have various substrate specificity and regioselectivity are discovered. Although *in vitro* assay using radiolabeled substrate and microsomal protein and *in vivo* assay with heterologous host were used for characterization of acyl-CoA desaturases, it is difficult to measure and compare the diverse functions of these enzymes exactly. So, I

attempted to construct the *in vitro* desaturation system by improving the detection method of acyl-CoA.

In chapter 4, I constructed the purification system of D6d and D5d for the crystal structure analysis. Cytochrome b_5 participates in desaturation reaction, which is one of the oxidation-reduction reactions, as the electron transport factor. Some of the desaturases, including D6d and D5d have cytochrome b_5-like domain with the heme-binding motif in their N or C terminal (Fig. 2). Our group elucidated both of this domain and diffused cytochrome b_5 in endoplasmic reticulum were necessary for expression of maximum activity of rat D6d (28). Although molecular mechanism of electron transportation between this domain and the catalytic center attracted our interest, the lack of information of three-dimensional structure prevents the elucidation of this mechanism. Thus, in order to achieve crystallization of D6d and D5d, I constructed mass production system of those desaturases with using methylotrophic yeast and examined the condition of desaturases solubilization and purification.

2. Identification of amino acid residues that determine the substrate specificity of mammalian membrane-bound front-end fatty acid desaturases.

2.1. Introduction

Fatty acid desaturases are oxidases that introduce a double bond in the acyl chain of a fatty acid substrate by removing 2 hydrogens from adjacent carbon atoms using active oxygen. They comprise 2 types. Water-soluble desaturases are found in cyanobacteria and higher plants, and act on the acyl chain bound to ACP (29), whereas membrane-bound desaturases from fungi, higher plants, and animals act on acyl-CoA or acyl-lipid substrates (30, 31). Some water-soluble enzymes such as castor Δ9 desaturase and ivy Δ4 desaturase are well characterized, and their crystal structures have revealed a molecular interaction between the ACP portion of the substrate and an amino acid located at the substrate-binding pocket of the enzyme, which could be the basis for change in the substrate specificity (32). The membrane-bound desaturases associate with endoplasmic reticulum membranes *via* 2 large hydrophobic domains that separate 3 hydrophilic clusters. The N-terminal hydrophilic region of some of these desaturases including mammalian Δ5 and Δ6 desaturases (D5d and D6d, respectively) and the C-terminal region of *Saccharomyces cerevisiae* Δ9 desaturase (OLE1p) contain a cytochrome b_5-like heme-binding His-Pro-Gly-Gly (HPGG) motif. The histidine residue is indispensable for electron transfer from NADH-dependent cytochrome b_5 reductase during the redox reaction (33, 34). Both this motif and that of diffused cytochrome b_5 are necessary to fully express desaturase activity (28, 35). The other hydrophilic regions contain 3 histidine clusters ($HX_{3-4}H$, $HX_{2-3}HH$, and $QX_{2-3}HH$) that form a catalytic center by coordinating non-heme diiron centers, and all of these histidine residues and the glutamine residue are essential for enzymatic activity (17, 21). D5d and D6d as well as Δ4 desaturase introduce a double bond at the respective Δ positions of fatty acid substrates between the carboxyl group and a pre-existing double bond; therefore, these enzymes are called “front-end” desaturases (36). They are distinct from

desaturases of ω-*x* and ν+*x* types that form double bonds at the methyl-terminal side.

The substrate specificity and regioselectivity (double bond positioning) of membrane-bound desaturases are defined by the structural fitness and interface affinity between the fatty acid substrate, including CoA and the lipid carrier, and the substrate-binding pocket with its surrounding residues. Protein engineering has been applied to understand the structure–function relationship. For instance, domain swapping has been used to identify the regioselective sites of nematode Δ12 and ω3 desaturases (37), a region determining the substrate specificity of *Aspergillus nidulans* Δ12 and ω3 desaturases (38), and a substrate recognition region of blackcurrant Δ6 fatty acid desaturase and Δ8 sphingolipid desaturase (39). Site-directed mutagenesis based on amino acid sequence comparison has been employed to identify amino acids participating in the substrate specificity of *Mucor rouxii* Δ6 desaturase (40), *Siganus canaliculatus* Δ4 and Δ5/6 desaturases (41), and marine copepod Δ9 desaturase (42). The regioselectivity of house cricket Δ12/Δ9 desaturase was investigated using chemical mutagenesis and yeast complementation assays (43). Moreover, fatty acid-modifying enzymes with protein structures similar to, but chemoselectivities different from, the fatty acid desaturases have been used to swap the function of *Arabidopsis* oleate 12-desaturase and hydroxylase (44), and to alter the product partitioning between *Crepis alpina* Δ12 desaturase and acetylenase (45) and *Momordica* conjugase itself (46).

In this study, we aimed to elucidate the structural basis of the substrate specificity of *Rattus norvegicus* D6d and D5d (13) by domain swapping and site-directed mutagenesis. The corresponding genes are positioned in a head-to-head configuration on the rat genome, suggesting a paralogous relationship (36). Although their primary structures are highly homologous, they are in charge of mutually exclusive substrates: D6d catalyzes the conversion of linoleic acid (LA; 18:2 Δ9,12) and α-linolenic acid (18:3 Δ9,12,15) into γ-linolenic acid (GLA; 18:3 Δ6,9,12) and stearidonic acid (18:4 Δ6,9,12,15), respectively, whereas D5d acts on dihomo-γ-linolenic acid (DGLA; 20:3 Δ8,11,14) and eicosatetraenoic acid (20:4 Δ8,11,14,17) to

generate arachidonic acid (ARA; 20:4 Δ5,8,11,14) and eicosapentaenoic acid (20:5 Δ5,8,11,14,17), respectively. To identify and evaluate the amino acid residues important for substrate selection of D6d, we performed additional analyses on the basis of the primary sequence of zebrafish bifunctional Δ5/6 desaturase (zD5/6d; (47)) and the recently reported crystal structure of human stearoyl-CoA (Δ9) desaturase (23, 48).

2.2. Experimental Procedures

2.2.1. Microorganisms, culture media, and reagents

Transformants of *Escherichia coli* DH5α were grown in Luria-Bertani (LB) medium (0.5% yeast extract, 1% NaCl, 1% Bacto tryptone, 2% agar for plates) or 2× yeast extract tryptone (YT) medium (1.6% Bacto tryptone, 1% yeast extract, 0.5% NaCl) supplemented with ampicillin (50 μg/ml) at 37°C with rotary shaking at 160 rpm. Transformants of *Saccharomyces cerevisiae* INVSc1 (Invitrogen, Carlsbad, CA) were selected on synthetic defined (SD) agar plates (0.67% yeast nitrogen base, 0.19% yeast synthetic dropout medium without uracil, 2% D-glucose, 2% agar) and cultivated in *Saccharomyces cerevisiae* transformant (SCT) medium (0.67% yeast nitrogen base, 0.19% yeast synthetic dropout medium without uracil, 4% raffinose, 0.1% Tergitol) or yeast extract polypeptone dextrose (YPD) medium (2% polypeptone, 1% yeast extract, 2% D-glucose) at 28°C and 160 rpm. Fatty acids were purchased from Sigma-Aldrich (St. Louis, MO) or Cayman Chemical (Ann Arbor, MI). Other guaranteed reagents were obtained from Nacalai Tesque (Kyoto, Japan), Sigma-Aldrich, Toyobo (Osaka, Japan), or Wako Chemicals (Osaka, Japan), unless otherwise indicated.

2.2.2. Construction of plasmids carrying desaturase genes

A FLAG DNA fragment was synthesized by PCR amplification with Takara Ex Taq (Takara, Kyoto, Japan) and the oligonucleotide primers FLAGf and FLAGr (Table 1), using 10 cycles of 95°C for 30 sec, 50°C for 30 sec, and 74°C for 30 sec, without template. The fragment was subcloned in pGEM-T Easy vector (Promega, Madison, WI) and transformed into *E. coli* DH5α (pGEM-FLAG). The rat D6d gene (DDBJ accession number AB021980) was amplified from stock plasmid with KOD-Dash DNA polymerase (Toyobo) and the primers 24aF+ and 24R+ (Table 1), using 30 cycles of 95°C for 30 sec, 68°C for 2 sec, and 74°C for 30 sec, and was digested with *Kpn* I and *Xba* I. The product was ligated into *Kpn* I/*Spe* I-digested

pGEM-FLAG and the plasmid was transformed into *E. coli* DH5α (pGEM-FLAG-D6d). The rat D5d gene (DDBJ accession number AB052085) was amplified using KOD polymerase (Toyobo), the primers rD5df and rD5dr (Table 1), and a rat liver cDNA library (Clontech Laboratories, Palo Alto, CA) under the same thermal cycling conditions as for D6d, and was ligated into pGEM-FLAG (pGEM-FLAG-D5d). The nucleotide sequences of all plasmids were determined using the DYEnamic ET terminator cycle sequencing kit (GE Healthcare, Buckinghamshire, UK) or BigDye Terminator v3.1 cycle sequencing kit (Life Technologies, Carlsbad, CA) with T7, SP6, and other appropriate primers (Table 1) on an ABI PRISM 310 or 3130x1 genetic analyzer (Life Technologies).

2.2.3. Construction of chimeric desaturase genes

DNA fragments corresponding to the N-terminal region (cyt) and the central and C-terminal regions (des) of D6d (D6cyt and D6des) and D5d (D5cyt and D5des) were amplified by PCR using KOD Dash, the template plasmids, and the following sets of oligo primers (Table 1): D6cyt (aa 1–154), 24aF+ and D6d-cytr; D6des (aa 155–444), D6d-cytrf and 24R+; D5cyt (aa 1–156), D5df and D5d-cytr; and D5des (aa 157–447), D5d-cytf and D5dr. The products were digested with *Sac* II at the coupling site, incubated at 70°C for 15 min to inactivate the enzyme, and ligated with T4 DNA ligase in the following combinations: D6cyt-D6des, D6cyt-D5des, D5cyt-D6des, and D5cyt-D5des. Each of the resultant fragments was adenylated with Ex Taq (Takara) at 72°C for 10 min, subcloned into the pGEM-T Easy vector, digested with *Kpn* I and *Sal* I, and ligated into pGEM-FLAG.

2.2.4. Site-directed mutagenesis

The oligonucleotide primers d6d5-1–d6d5-48 and d6zebd5-1–d6zebd5-20 (Table 1) were designed to introduce nucleotide mutations for substitution of amino acids in D6d and D5d with each of their D5d, zD5/6d, or D6d counterparts (see Fig. 3). Each mutation site was

flanked by at least 15 nucleotides in each primer. For multiple-site mutagenesis, 3 or 4 primers carrying mutation site(s) at least 15 amino acid residues apart from each other were mixed in an equivalent molar ratio. The primers were phosphorylated at the 5′ end with T4 polynucleotide kinase (Takara). Plasmids carrying single or multiple mutation(s) were synthesized using pGEM-FLAG-D6d or pGEM-FLAG-D5d as a template, the phosphorylated primers, and the QuikChange multi site-directed mutagenesis kit (Agilent Technologies, Santa Clara, CA) or a combination of the AMAP multi site-directed mutagenesis kit (MBL International, Woburn, MA) and Pfu DNA polymerase (Thermo Scientific Fermentas, Carlsbad, CA), according to the manufacturer's instructions. The reaction mix was used to transform *E. coli* DH5α or XL10-Gold ultracompetent (Agilent Technologies) cells and transformants were randomly selected to check the nucleotide sequences of the cloned DNA fragments.

Table 1. Oligonucleotide primers used in this study.

Primer	Nucleotide sequence (5' to 3' direction)	Purpose[a]
Preparation of whole and partial regions of desaturases		
FLAGf	GCAAAGCTTAAGATGGACTATAAGGATGATGATGAC	FLAG tag
FLAGr	CGTGGTACCCTTGTCATCATCATCCTTATAG	FLAG tag
24aF+	ACAGGTACCATGGGGAAGGGAGGTAACCAG	D6d
24R+	GTCTCTAGATTCATTTGTGGAGGTAGGCATCC	D6d
D5df	CCCGGTACCATGGCTCCCGACCCGGTGCAGACCC	D5d
D5dr	CCCCTGCAGCTATTGGTGAAGGTAAGCATCCAGCC	D5d
D6d-cytr	GGGCCGCGGAAGTACGAGAGGATGAACC	N-terminal region of D6d
D6d-cytf	CCCTTCCGCGGCAATGGCTGGATTCCC	Middle and C-terminal regions of D6d
D5d-cytr	GGGTTCCGCGGAAGATCCAAAGAGTGAGC	N-terminal region of D5d
D5d-cytf	CCCTTCCGCGGAACTTCCTTGGTGCCC	Middle and C-terminal regions of D5d
Amino acid substitution of D6d with D5d		
d6d5-1	ACCGTCATCACGGCCGTTCTGCTTGCTACCTCCC	F166V, V167L
d6d5-2	ACGGCCTTTGTCCTTTCTACCGTCCAGGCCCAAGCTGGA	A169S, S171V
d6d5-3	GGCTACAACATGATTTTGGCCACCTTTCTGT	Y182F
d6d5-4	GCCACCTTTCTGTCTTTAGCACCTCCATATGGAAC	Y188F, K189S, K190T
d6d5-5	TTTCTGTCTATAAGAAATCCACATGGAACCACATTGTC	I192T
d6d5-6	TCCATATGGAACCACCTTGTCCACCATTTTGTCATTGGCCACTT	I196L, K199H
d6d5-7	CACTTAAAGGGTGCCCCCGCCAGCTGGTGGAACCATCG	S209P, N211S
d6d5-8	AACTGGTGGAACCATATGCATTTCCAGCACCAT	R216M
d6d5-9	CATGCGAAGCCCAACTGCTTCCGCAAGGACCCCGACAT	I226C, H228R
d6d5-10	GGACCCCGACATAAACATGCACGTGTTTGTCC	K234N, S235M, L236Δ
d6d5-11	ATAAAGAGCCTGCACCCATTGGTGTTTGTCCTTGGA	Δ238P, Δ239L
d6d5-12	ATAAAGAGCCTGCACTTCTTTGCCCTTGGAGAGTGGCA	V238F, V240A
d6d5-13	GTGTTTGTCCTTGGAAAGGTGCTGCCCCTCGAGTATGG	E243K, W244V, Q245L
d6d5-14	CTTGGAGAGTGGCAGTCCGTCGAGCTTGGCAAGAAGAAGCTG	P246S, L247V, Y249L
d6d5-15	CTCGAGTATGGCAAGGAGAAGAAGAAATATCTGCCCTA	K252E, L254K
d6d5-16	AAGAAGAAGCTGAAACATATGCCCTACAACCACC	Y256H, L257M
d6d5-17	TACAACCACCAGCATAAATACTTCTTCCTGA	E264K
d6d5-18	ATCTTGGGAGCCCTGTGTCTTTTCAACTTTATCAGGT	V321C, F322L, L323F
d6d5-19	GCCCTGGTTTTCCTCTTCATTGTCAGGTTCCTGGAGA	N324F, F325I, I326V
d6d5-20	AGGTTCCTGGAGAGCAACTGGTTTGTGTGGG	H332N
d6d5-21	CAGATGAACCACATTCCCATGCACATTGATCTTGATCAC	V344P, E346H
d6d5-22	TCATGGAGATTGATCATGATCGCTACCGGGACTGGTTCA	L349H, H351R
d6d5-23	ATTGATCTTGATCACAACGTGGACTGGTTCAGCAGC	Y352N, R353V
d6d5-24	CACTACCGGGACTGGGTCAGCACCCAGCTGGCAGCCAC	F356V, S358T
d6d5-25	TTCAGCAGCCAGCTGCAAGCCACCTGCAATGT	A361Q
d6d5-26	GCCACCTGCAATGTGCACCAGTCCTTCTTCA	E367H
d6d5-27	AATGTGGAGCAGTCCGCCTTCAATAACTGGTTCAGCGGGC	F370A, D373N
d6d5-28	TGCCAAGACACAACTACCACAAGGTTGCCCCACTGGTGA	L396Y, I399V
d6d5-29	AAGATTGCCCCACTGGTGCAGTCTCTCTGCGCCA	K404Q

d6d5-30	TCTCTCTGCGCCAAGTATGGCATTAAATACCAAGAGAAGC	H410Y, E413K
d6d5-31	CATGGCATTGAATACGAATCGAAGCCGCTGCTGAG	Q415E, E416S
d6d5-32	AGAAGCCGCTGCTGACGGCCTTCGCCGACATTGTGAGTTC	R421T, L423F, L424A
d6d5-33	CTGCTCGACATTGTGTATTCACTGAAGAAGTC	S428Y
d6d5-34	GTGAGTTCACTGAAGGAGTCTGGGCAGCTGTGGCTGGATG	K432E, E435Q
d6d5-35	GATGCCTACCTCCACCAATGAATCTAGTGAA	K444Q
Amino acid substitution of D5d with D6d		
d6d5-36	CACTTAAAGGGTGCCTCCGCCAGCTGGTGGAAC	P209S
d6d5-37	AGGGTGCCCCCGCCAACTGGTGGAACCAT	S211N
d6d5-38	CTGGTGGAACCATCGACATTTCCAGCACCAT	M216R
d6d5-39	GGACCCCGACATAAAGATGCACCCATTGGTGT	N234K
d6d5-40	ACCCCGACATAAACAGCCACCCATTGGTGTTTG	M235S
d6d5-41	CCGACATAAACATGCTGCACCCATTGGTGTTTG	Δ236L
d6d5-42	ATAAACATGCACTTGGTGTTTGTCCTTGGA	P238Δ
d6d5-43	ATAAACATGCACCCAGTGTTTGTCCTTGGA	L239Δ
d6d5-44	GTGTTTGTCCTTGGAGAGGTGCTGCCCCTCGA	K243E
d6d5-45	TTTGTCCTTGGAAAGTGGCTGCCCCTCGAGTA	V244W
d6d5-46	GTCCTTGGAAAGGTGCAGCCCCTCGAGTATGG	L245Q
d6d5-47	CAGATGAACCACATTGTCATGCACATTGATCTT	P344V
d6d5-48	AACCACATTCCCATGGAGATTGATCTTGATCAC	H346E
Amino acid substitution of D6d with zebrafish D5/6d		
d6zebd5-1	TCGTACTTCGGCACTGGCTGGATTCCC	N156T
d6zebd5-2	ACCGTCATCACGGCCGTTGTCCTTGCTACCTCC	F166V
d6zebd5-3	TGGCTACAACATGATTTCGGCCACCTTTCTGTC	Y182F
d6zebd5-4	CACCTTTCTGTCTTCAAGACCTCCATATGGAAC	Y188F, K190T
d6zebd5-5	TCCATATGGAACCACCTCGTCCACAAGTTTGTC	I195L
d6zebd5-6	GGACCCCGACATAAATATGCTGCACGTGTTTG	K234N, S235M
d6zebd5-7	CTTGGAGAGGTCCAGCCCGTCGAGTATGGC	W245V, L248V
d6zebd5-8	AAGAAGAAGCTGAAACACCTGCCCTACAACCAC	Y257H
d6zebd5-9	TACAACCACCAGCATAAGTACTTCTTCCTGATC	E265K
d6zebd5-10	TCCAGTACCAGATCTTCATGACCATGATCAG	I284F
d6zebd5-11	GCCATCAGCTACTATGTTCGTTTCTTCTACACC	A305V
d6zebd5-12	TTGGGAGCCCTGGTTCTCTTCAACTTTATCAGGTTC	F322L, L323F
d6zebd5-13	GTTTTCCTCAACTTTGTCAGGTTCCTGGAGAGC	I326V
d6zebd5-14	CAGATGAACCACATTCCCATGGAGATTGATCTTG	V344P
d6zebd5-15	ATTGATCTTGATCACAACCGGGACTGGTTCAGCAG	Y352N
d6zebd5-16	AATGTGGAGCAGTCCGCCTTCAATGACTGGTTC	F370A
d6zebd5-17	TGCCAAGACACAACTATCACAAGATTGCCCC	L396Y
d6zebd5-18	CTCTGCGCCAAGTACGGCATTAAGTACCAAGAGAAG	H410Y
d6zebd5-19	GCCAAGTACGGCATTAAATACCAAGAGAAGCCG	E413K
d6zebd5-20	CGCTGCTGAGGGCCTTCGCTGACATTGTGAGTTC	L423F, L424A

[a] Amino acids are indicated by single characters. Δ indicates a gap in the amino acid sequence alignment.

2.2.5. Expression of desaturase genes in yeast

The wild-type, chimera, and mutant desaturase genes were obtained by digestion of the pGEM-based plasmids with *Hin*d III and *Eco*RI and were ligated into the yeast expression vector pYES2 (Invitrogen). The desaturase expression vectors were introduced into *S. cerevisiae* INVSc1 by using the lithium acetate method (49). Transformants were selected on uracil-deficient SD plates and cultivated at 28°C for 6 h with rotary shaking at 160 rpm in 15 ml of SCT medium supplemented with LA or DGLA at a concentration of 0.25 mM. After addition of galactose (2%, w/v) and further cultivation for another 16 h, yeast cells were recovered by centrifugation for fatty acid and protein analyses.

2.2.6. Fatty acid analysis

The yeast cells from ~15 ml of broth were washed with distilled water and then vigorously vortexed in 2 ml of chloroform/methanol (2:1, v/v) plus 0.5 ml of distilled water. The chloroform phase was recovered by centrifugation, and methanolysis of total lipid was carried out by adding 1 ml of 10% methanolic hydrochloric acid (Tokyo Kasei, Tokyo, Japan) and heating at 60°C for 2 h. After evaporation of the solvents, fatty acid methyl esters (FAMEs) were extracted twice and dissolved in hexane. Fatty acid composition was determined using a gas chromatographic system (GC-17A and GC-2014, Shimadzu, Kyoto, Japan) equipped with a capillary column (TC-70; 0.25 mm × 30 m, GL Sciences, Tokyo, Japan, or Omegawax 250; 0.25 mm × 30 m, Sigma-Aldrich), a split injector (split ratio at 1:20–25; 270°C), and a flame ionization detector (270°C). The temperature of the column oven was maintained at 180°C (TC-70) or raised from 210°C to 225°C at 0.5°C/min (Omegawax 250). FAMEs were identified by comparing their retention time with those of the 37-Component FAME mix (Supelco, Bellefonte, PA) and by analyzing their molecular mass using mass spectrometry (MS). For gas chromatography (GC)-MS analysis, total-lipid or FAME extracts were dissolved in 0.5 ml of 2-amino-2-methyl-1-propanol preheated at 75°C and were heated at 180°C for 24 h to form

4,4-dimethyloxazoline (DMOX) derivatives of fatty acids. After cooling to 75°C and adding 2 ml of distilled water preheated at 75°C, the DMOX derivatives were extracted several times with *n*-hexane/dichloromethane (2:3, v/v), dehydrated with anhydrous sodium sulfate, and analyzed on a GC-MS system consisting of a gas chromatograph (7890A, Agilent Technologies) equipped with a ZB-1HT Inferno capillary column (0.25 mm × 30 m, Phenomenex, Torrance, CA) and an electron ionization mass spectrometer (70 eV, JMS-T100GCV; JEOL, Tokyo, Japan). The enzymatic activity of the desaturase expressed in yeast was evaluated using the conversion ratio, which was determined as the ratio of the amount of product to the sum of the amounts of substrate and product and was expressed as a percentage.

2.2.7. SDS-PAGE and western blotting

Yeast cells recovered from 1 ml of broth were washed with distilled water and suspended in 0.1 ml of 50 mM Tris-HCl (pH 7.5) containing 4 µl EDTA-free protease inhibitor cocktail (Roche, Basel, Switzerland). An equivalent volume of glass beads (0.5 mm in diameter) was added to disrupt the cells by eight rounds of vortexing for 30 sec and chilling on ice for 30 sec. The homogenate was centrifuged at 5000 × *g* for 10 min and the supernatant was subjected to SDS-PAGE (50). The proteins separated in the gel were transferred to an Immobilon membrane (Merck Millipore, Darmstadt, Germany) using a semi-dry blotter. The membrane was blocked by immersing in 5% skim milk in PBST (137 mM NaCl, 2.7 mM KCl, 10 mM Na_2HPO_4, 1.76 mM KH_2PO_4, 0.05% (w/v) Tween-20), and then moved to the same buffer containing mouse anti-FLAG antibody (Sigma-Aldrich; 1:5000). After shaking for 1 h and washing with PBST, the membrane was probed with rabbit anti-mouse IgG (1:20000) for 1 h. The FLAG-tagged proteins were detected by using ECL plus (GE Healthcare) and exposure to X-ray film.

2.2.8. Statistical analysis

All experiments were performed at least twice. Student's *t*-test was used to compare experimental values between groups where applicable. $P < 0.05$ was considered significant.

2.3. Results

2.3.1 The N-terminal region of desaturase is not involved in substrate specificity

To examine the involvement of the N-terminal hydrophilic regions of D6d and D5d, including the cytochrome b_5-like domain, in the substrate specificity of both desaturases, chimeras D5cyt-D6des and D6cyt-D5des were constructed and expressed in yeast in the presence of LA or DGLA. The results indicated that D5cyt-D6des and D6cyt-D6des converted LA into GLA, but did not act on DGLA, whereas D6cyt-D5des and D5cyt-D5des generated ARA from DGLA, but did not use LA as a substrate (Table 2). No other fatty acids, except spontaneous ones, were detected in all cases (data not shown). These results indicated that the N-terminal domains of both enzymes do not determine the specificity toward the corresponding substrates. However, the rate of conversion by D5cyt-D6des (8%) was substantially lower than that by D6cyt-D6des (40%), suggesting that a specific interaction between the N-terminal region and the central and C-terminal regions may contribute to maximum activity of D6d through conformational stabilization of the enzyme.

Table 2. Substrate specificity of chimeric desaturases.

Desaturase	Rate of substrate conversion (%)	
	LA to GLA	DGLA to ARA
D6cyt-D6des	40	0
D5cyt-D6des	8.0	0
D6cyt-D5des	0	45
D5cyt-D5des	0	45

2.3.2. Identification of amino acids responsible for D6d activity

The amino acid sequence homology between D6d and D5d was 66% (67/101 amino acids) in the central hydrophilic region (Hydrophilic region II) and 73% (91/124) in the C-terminal region (Hydrophilic region III). To identify the amino acids involved in substrate specificity, site-directed mutagenesis was applied to the 67 non-identical amino acids, which had been organized into 35 groups of 1–3 amino acid substitutions as depicted in Fig. 3.

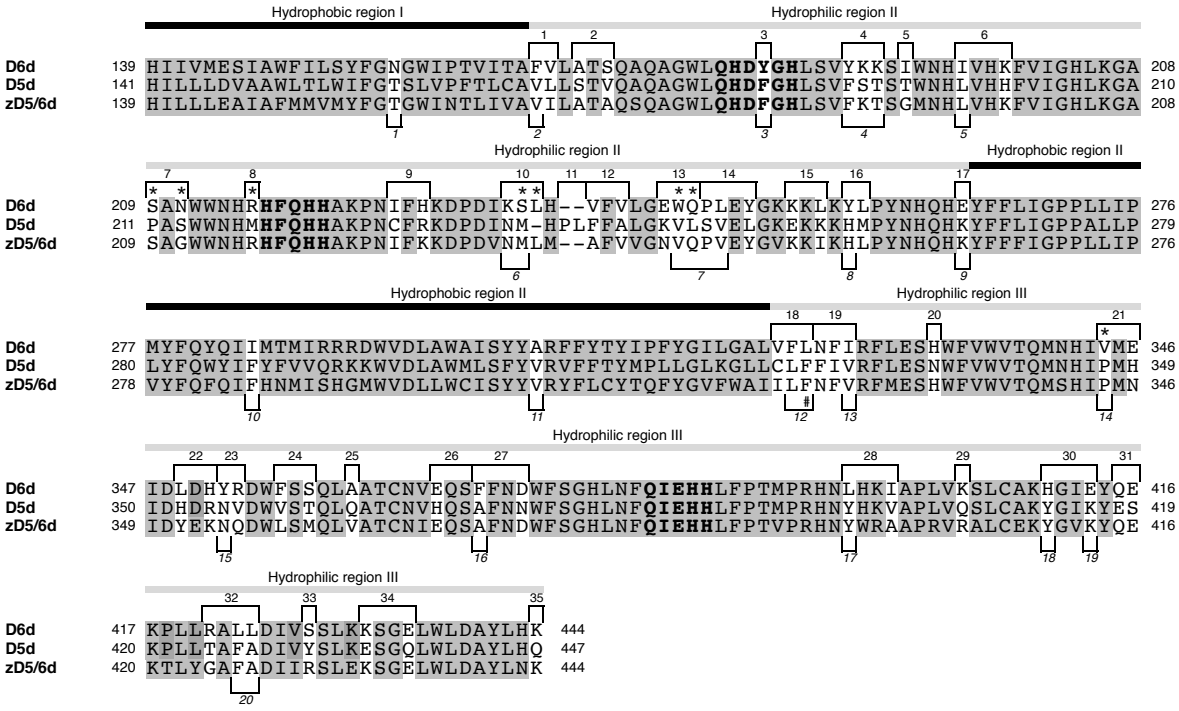

Figure 3. Alignment of the amino acid sequences of rat D6d and D5d and zebrafish zD5/6d. Site-directed mutagenesis was applied to create mutations at the sites shown with a white background using oligonucleotide primers indicated by respective numbers above (d6d5-1– d6d5-35) and below (d6zebd5-1– d6zebd5-20) the alignment. Conserved histidine clusters are indicated by bold letters. Asterisks indicate mutation sites that altered the substrate specificity from D6d-type to D5d-type. "#" indicates the mutation site that gave rise to Δ5/6 bifunctionality of D6d.

Multi site-directed mutagenesis using mixtures of 3 or 4 groups of oligonucleotide primers (d6d5-1–d6d5-35; Table 1) resulted in the generation of an array of mutant D6d genes encoding enzymes in which various (numbers of) amino acids were substituted with the corresponding D5d residues (Fig. 4). The mutant genes were individually expressed in *S. cerevisiae* in the presence of DGLA. In spite of the successful expression of mutant proteins, none of the mutants generated ARA at a detectable level (data not shown). A series of expression experiments was then performed in the presence of LA to see whether the D6d activity of the mutants had been changed. As shown in Fig. 4, the D6d activity of 4 mutants constructed using the primer sets d6d5-1/11/25 (introducing the mutations F166V+V167L, Δ238P+Δ239L, A361Q), d6d5-5/10/35 (I192T, K234N+S235M+L236Δ, K444Q), d6d5-7/23/30 (S209P+N211S, Y352N+R353V, H410Y+E413K), and d6d5-8/14/24/31 (R216M,

P246S+L247V+Y249L, F356V+S358T, Q415E+E416S) was significantly lower than that of intact D6d. Further analysis of the mutants generated by using fewer or single primer(s) revealed that the amino acid change(s) introduced by each of the primers d6d5-7 (S209P+N211S), d6d5-8/31 (R216M, Q415E+E416S), d6d5-10/35 (K234N+S235M+L236Δ, K444Q), and d6d5-11 (Δ238P+Δ239L), yielded decreased or null D6d activity. Since the single primer mutations d6d5-31 and d6d5-35 did not affect to the D6d activity, the decreases in the activity by the mutations d6d5-8/31 and d6d5-10/35 could be due to the mutations by d6d5-8 and d6d5-10, respectively.

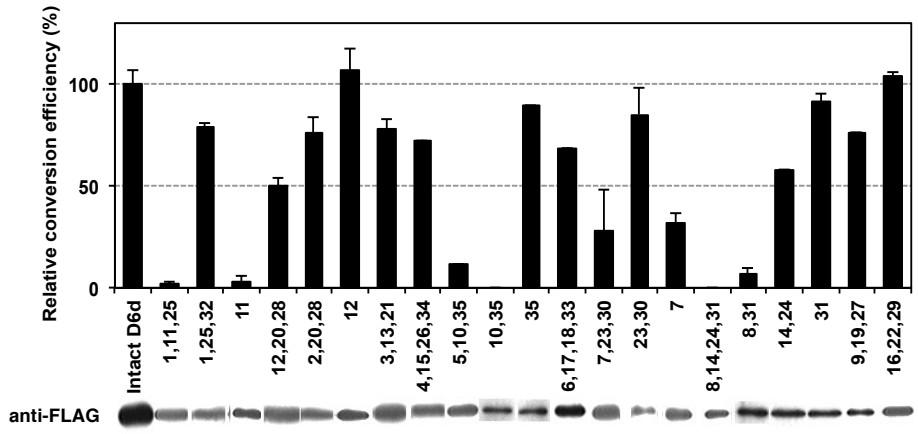

Figure 4. Δ6 desaturase activity of D6d mutants. The D6d mutants were generated by site-directed mutagenesis using one or more oligonucleotide primers as indicated by the numbers, which correspond with the primer numbers (d6d5-1–d6d5-35; Table 1). The mutants carrying D5d amino acid(s) were expressed in yeast *S. cerevisiae* in the presence of LA and the fatty acid composition was measured as described in the Experimental procedures. D6d activity was determined as the conversion rate from LA to GLA and is shown as the average value relative to that of intact D6d, together with the standard deviation (n = 3). FLAG-tagged D6d proteins were detected by western blotting of total yeast protein using anti-FLAG antibody.

2.3.3. Switching the substrate specificity of D6d

As expected, a D6d mutant made by using a mixture of the 4 primers d6d5-7, 8, 10, and 11 showed neither D6d nor D5d activity. Additional mutations were introduced into this mutant using several sets of primers randomly selected from d6d5-1– d6d5-35, and D5d activity of the resultant mutants was investigated using DGLA substrate. Figure 5D shows that one D6d mutant, namely, D6d-Z2, made using the primers d6d5-13 (E243K+W244V+Q245L) and

d6d5-21 (V344P+E346H) in addition to d6d5-7/8/10/11 (S209P+N211S, R216M, K234N+S235M+L236Δ, Δ238P+Δ239L), gave a peak with a retention time similar to that of ARA (peak 6, Fig. 5D) on the chromatogram. By GC-MS analysis of its DMOX derivative, the generated fatty acid was identified as ARA on the basis of its total mass (*m*/*z* = 357), the MS pattern of fragment ions, and a mass peak at *m*/*z* = 153, characteristic of a Δ5 double bond (Fig. 5E). The conversion efficiency from DGLA to ARA of D6d-Z2 was 12% of that of intact D5d, whereas the efficiencies of the mutants made using the primers d6d5-13 (E243K+ W244V+Q245L) and d6d5-21 (V344P+E346H) were 8% and 2%, respectively. Other mutants made by using the primer sets d6d5-2/30 (A169S+S171V, H410Y+E413K), d6d5-5/16/24/33 (I192T, Y256H+L257M, F356V+S358T, S428Y), and d6d5-19/26/28 (N324F+F325I+I326V, E367H, L396Y+I399V), also generated ARA from DGLA; however, the efficiency was less than 2% of that of D5d in all cases. Because the enzymes carrying the mutations introduced by d6d5-13 (E243K+W244V+Q245L) showed the highest D5d activity and only the mutations introduced by d6d5-21 (V344P+E346H) were located at the C-terminal region of D6d, the mutant D6d-Z2, possessing both of those mutated regions, was used for further analysis.

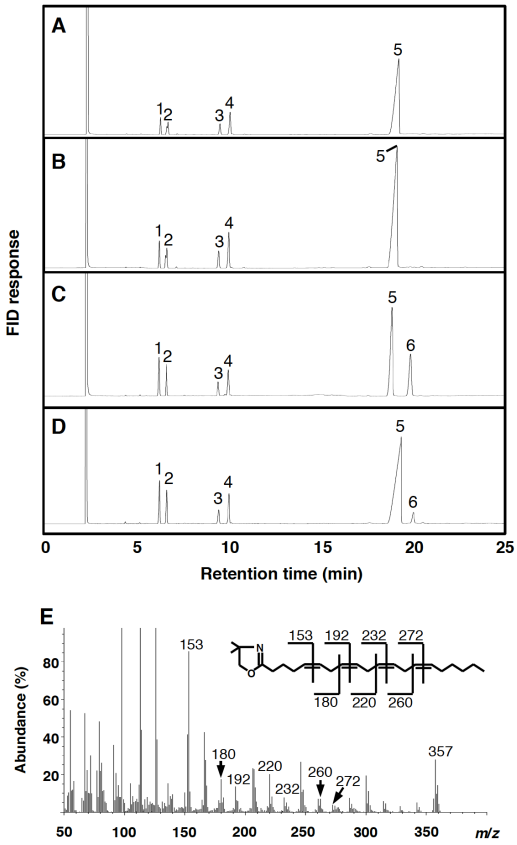

Figure 5. Conversion of ARA from DGLA by D6d desaturase mutant D6d-Z2 carrying 12 D5d amino acids. Intact D6d (panel B), intact D5d (panel C) and D6d-Z2 (panel D) were expressed in yeast in presence of DGLA (20:3 Δ8,11,14; peak 5), and the generation of ARA (20:4 Δ5,8,11,14; peak 6) was detected by GC. Yeast harboring the pYES2 vector was used as negative control (panel A). Other peaks in panels A–D are 16:0 (peak 1), 16:1 Δ9 (peak 2), 18:0 (peak 3), and 18:1 Δ9 (peak 4). DMOX-derivative of ARA generated by the mutant D6d-Z2 (peak 6 in panel D) was identified by GC-MS analysis (panel E) as described in the Experimental procedures. Predicted molecular mass numbers of daughter ions of ARA are shown on the structural formula.

To exclude the mutations that do not contribute to the D5d activity of D6d-Z2, each of its 12 D5d amino acids was restored to its D6d counterpart by using the primers d6d5-36–d6d5-48. Expression analysis of the restored mutants in yeast revealed that mutations P209S, S211N, M216R, M235S, Δ236L, V244W, L245Q, and P344V decreased the D5d activity compared to that of D6d-Z2, while the mutations L239Δ and H346E boosted the activity (Fig. 6A). Thus, a new D6d mutant, namely, D6d-mut8, carrying the 8 mutations S209P, N211S, R216M, S235M, L236Δ, W244V, Q245L, and V344P, was made and expressed in yeast in the presence of DGLA (Fig. 6B). The D5d activity of D6d-mut8 was 1.4%, equivalent to 30.1% and 4.7% of that of D6d-Z2 and intact D5d, respectively (Figs. 5 and 6B). Another D6d mutant

carrying the substitutions R216M and W244V that yielded the lowest activity in the restoration experiment (Fig. 6A) was made, and its activity was examined. Although a fatty acid with a retention time similar to that of ARA was detected, GC-MS analysis did not allow structural identification due to an insufficient amount of fatty acid (data not shown).

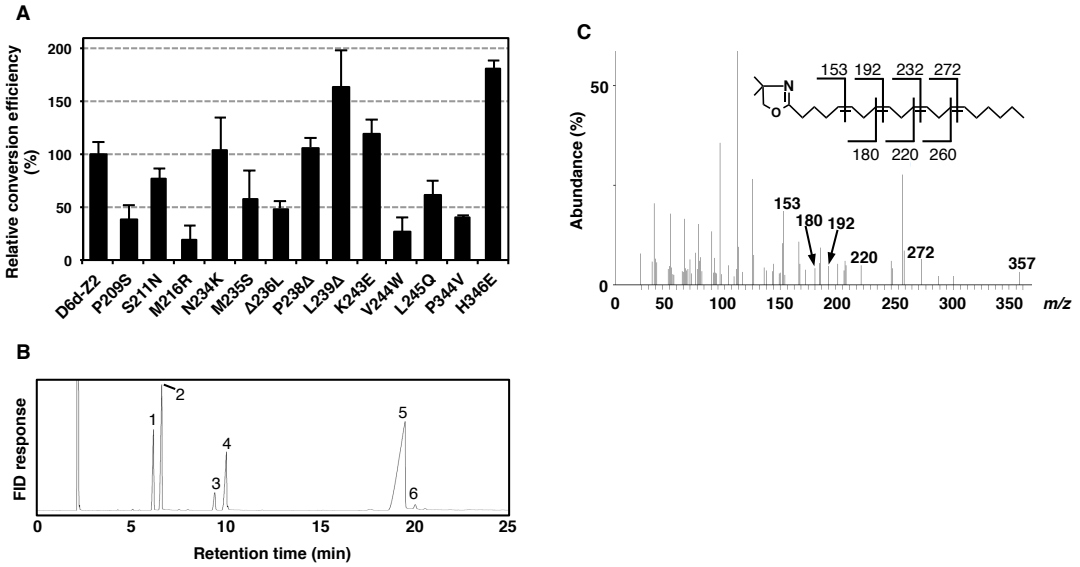

Figure 6. Δ5 desaturase activity of point mutants obtained from D6d-Z2. A, Each of D5d amino acid changes or the gap in D6d-Z2 was restored to its D6d counterpart by site-directed mutagenesis using oligonucleotide primers (d6d5-36– d6d5-48; Table 1). The mutants were expressed in yeast in the presence of DGLA, and the generation of ARA was detected by GC. D5d activity was determined as the conversion rate of DGLA to ARA and shown as the average value relative to that of D6d-Z2, together with the standard deviation (n = 3). B, D6d-mut8 carrying eight D5d-type amino acids was expressed in yeast in the presence of DGLA (peak 5), and the generation of ARA (peak 6) was detected by GC. Other peaks in panel B are 16:0 (peak 1), 16:1 Δ9 (peak 2), 18:0 (peak 3), and 18:1 Δ9 (peak 4). C, GC-MS analysis of DMOX derivatives of the fatty acid (peak 6 in B) produced by the mutant D6d-mut8.

2.3.4. Mutations conferring bifunctionality to D6d

The swapping of different amino acids within D6d with their D5d counterparts provided D6d with D5d activity as mentioned above; however, D6d activity was lost (data not shown). Thus, the rat desaturases were compared with the bifunctional Δ5/Δ6 desaturase from zebrafish (zD5/6d), which acts on both LA and DGLA (47). Twenty-five amino acids shared by D5d and zD5/6d, but not by D6d (Fig 3), were selected as target sites for mutation. A D6d mutant carrying the 25 corresponding D5d and zD5/6d amino acids, namely, D6d-25m, was made by multi site-directed mutagenesis using the oligonucleotide primers d6zebd5-1–

d6zebd5-20 (Table 1). I examined its substrate specificity using the yeast expression system and GC-MS analysis. D6d-25m could act on both LA and DGLA to generate GLA and ARA at conversion rates of 26.3% and 6.8%, respectively (Fig. 7, Table 3), proving the acquisition of D5d activity without losing D6d activity.

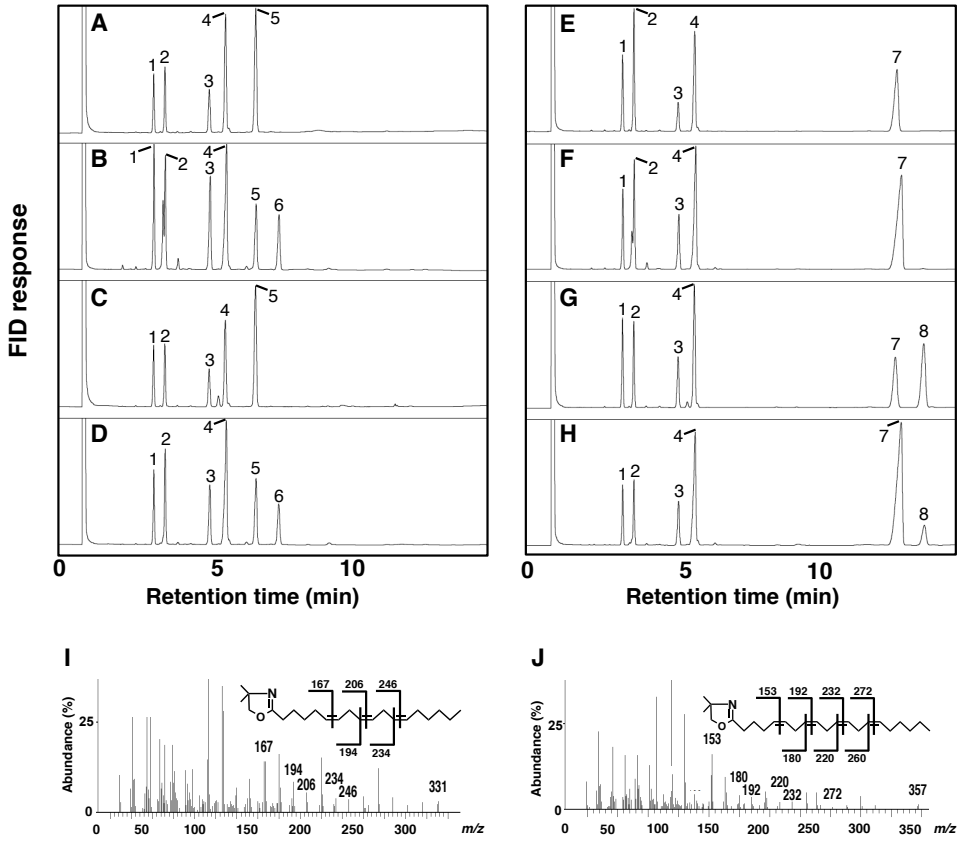

Figure 7. Fatty acid analysis of desaturation products of mutant D6d-25m. Null vector pYES2, intact D6d, intact D5d and D6d-25m were expressed in yeast in the presence of LA (peak 5; panels A-D) or DGLA (peak 7; panels E-H), and the fatty acid composition of total cellular lipids was analyzed by GC. Each panel is null vector + LA (A), intact D6d + LA (B), intact D5d + LA (C), D6d-25m + LA (D), null vector + DGLA (E), intact D6d + DGLA (F), intact D5d + DGLA (G) and D6d-25m + DGLA (H). Other peaks in panels A–H are 16:0 (peak 1), 16:1 Δ9 (peak 2), 18:0 (peak 3), 18:1 Δ9 (peak 4), 18:3 Δ6,9,12 (peak 6) and 20:4 Δ5,8,11,14 (peak 8). Mass spectra of DMOX derivatives of fatty acids generated by D6d-25m expressed in yeast in the presence of LA (panel I; peak 6 in panel D) or DGLA (panel J; peak 8 in panel H). Predicted molecular masses of daughter ions of GLA and ARA are shown on the respective structural formulas in panels I and J.

Table 3. D5d and D6d activities of D6d mutants carrying zebrafish D5/6d-type amino acids.

Substitution	1C-1	1C-2	1C-3	2C-1	2C-2	2C-3	2C-4	3C-1	3C-2	3C-3	4C-1	4C-2	4C-3	4C-4	5C-1	D6d 25m
N156T	+	+	+	+	+	+	+	+	+	+	+	+	+	+	+	+
A305V	+	+	+	+	+	+	+	+	+	+	+	+	+	+	+	+
Y182F		+	+	+	+	+	+	+	+	+	+	+	+	+	+	+
K234N		+	+	+	+	+	+	+	+	+	+	+	+	+	+	+
S235M		+	+	+	+	+	+	+	+	+	+	+	+	+	+	+
E365K			+	+	+	+	+	+	+	+	+	+	+	+	+	+
F166V				+	+	+	+	+	+	+	+	+	+	+	+	+
L423F				+		+	+	+	+	+	+	+	+	+	+	+
L424A				+		+	+	+	+	+	+	+	+	+	+	+
L248V				+			+	+	+	+	+	+	+	+	+	+
F322L					+	+	+	+	+	+	+	+	+	+	+	+
L323F					+	+	+	+	+	+	+	+	+	+	+	+
I195L							+	+	+	+	+	+	+	+	+	+
W245V							+	+	+	+	+	+	+	+	+	+
L396Y								+	+	+	+	+	+	+	+	+
Y257H								+		+	+	+	+	+	+	+
V344P									+	+	+	+	+	+	+	+
I284F										+	+	+	+	+	+	+
F370A											+	+		+	+	+
Y352N											+		+	+	+	+
I326V												+	+	+	+	+
Y188F														+	+	+
K190T														+	+	+
H410Y													+		+	+
E413K																+
D5d activity (%)	0	0	0	0	2.5	2.6	1.3	2.4	2.8	2.6	3.4	6.2	4.4	4.8	5.3	6.8
D6d activity (%)	16.3	17.4	13.7	5.3	11.6	10.0	13.5	13.0	13.0	16.0	13.8	11.0	21.3	21.3	26.8	26.3

+ indicates mutation points of each D6d mutant carrying zebrafish D5/6d-type amino acids.
D5d and D6d activities were represented as conversion rate from substrates (18:2 Δ9,12 for D6d and 20:3 Δ8,11,14 for D5d) to products (18:3 Δ6,9,12 for D6d and 20:4 Δ5,8,11,14 for D5d, respectively).

To determine the mutations responsible for the bifunctional nature of D6d-25m, 15 mutants harboring fewer mutations, obtained during D6d-25m construction, were examined for their D5d activity. A remarkable increase in D5d activity was observed by introducing the mutations F322L/L323F (mutant 2C-2), I326V (4C-2), and E413K (D6d-25m) to the respective backgrounds (Table 3). Further analysis of single mutants for each of these 4 amino acids introduced into wild-type D6d demonstrated that only L323F led to the generation of ARA from DGLA at a conversion rate of 2.3% (Fig. 8). Since addition of the mutations I326V and I326V/E413K to L323F did not significantly increase D5d activity, amino acids other than those might contribute to the full activity of D6d-25m.

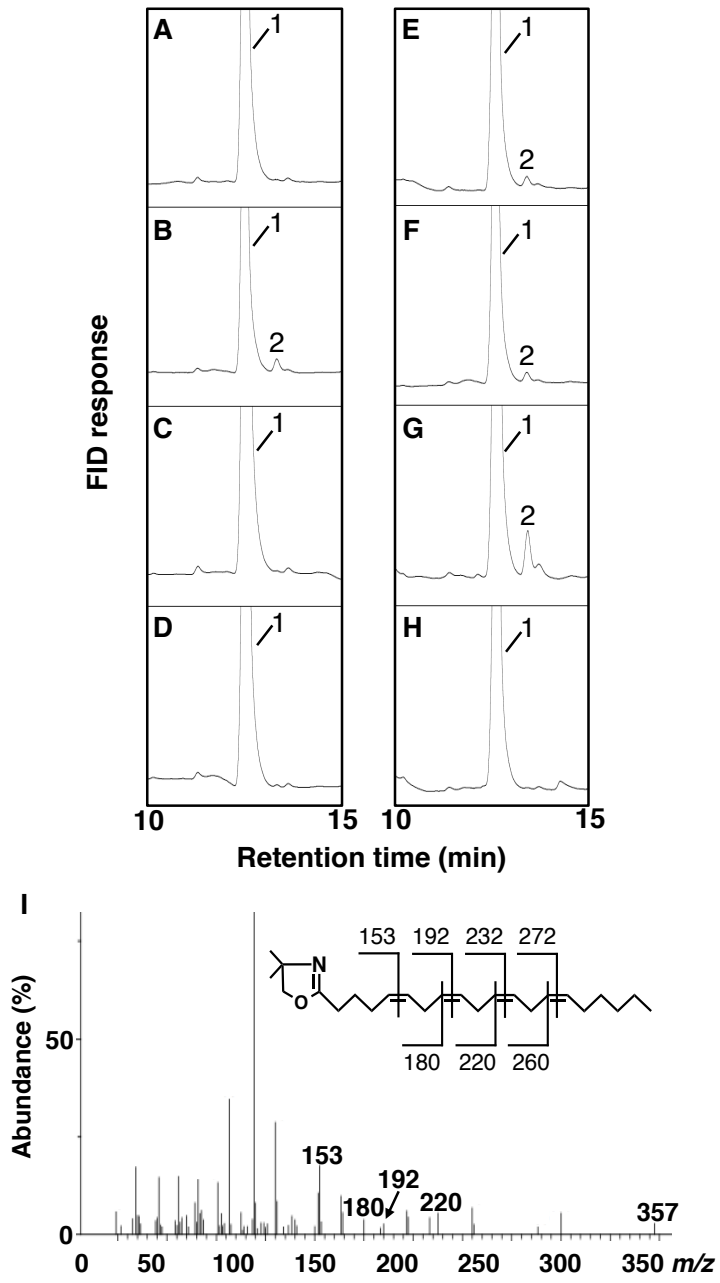

Figure 8. Conversion of ARA from DGLA by desaturase mutants with point mutation(s). A, D6d-F322L; B, D6d-L323F; C, D6d-I326V; D, D6d-E413K; E, D6d-L323F-I326V; F, D6d-L323F-I326V-E413K; G, D6d-25m; H, intact D6d. Each mutant was expressed in yeast in the presence of DGLA (peak 1), and the generation of ARA (peak 2) was detected by GC. I, GC-MS analysis of DMOX derivative of the fatty acid (peak 2 in B) produced by mutant D6d-L323F.

2.3.5. Structure-function relationship

To explore the molecular evolution and functional divergence of front-end fatty acid desaturases, the mutations that conferred D5d activity to D6d in this study were compared to the corresponding residues in desaturases from various vertebrates (27, 47, 51–56) as shown in Fig. 9. Most of the amino acids at positions 209, 211, 216, 236, and 245 of rat D6d are conserved among each group of D6d and D5d, and amino acids at those sites are D6d-type in teleost bifunctional desaturases. Therefore, these specificity-determining residues might be targets for functional modification of these types of desaturases. Further, the amino acids at positions 235 and 344 are highly conserved among D6d and D5d from most vertebrates, while those at positions 244 and 323 are variable. It is possible that these conserved amino acids cooperatively contribute to substrate recognition.

	Amino acid number								
	209	211	216	235	236	244	245	344	323
Rattus norvegicus D6d	S	N	R	S	L	W	Q	V	L
Homo sapiens D6d	S	N	R	M	L	W	Q	V	L
Gallus gallus D6d	S	N	R	M	L	S	Q	P	L
Scyliorhinus canicula D6d	S	N	R	M	L	V	Q	P	V
Salmo salar D6d	S	N	R	M	L	K	Q	P	I
Danio rerio D5/6d	S	G	R	M	L	V	Q	P	F
Siganus canaliculatus D5/6d	S	N	R	M	V	T	Q	P	I
Salmo salar D5d	S	N	R	S	L	T	Q	P	I
Scyliorhinus canicula D5d	P	S	L	M	H	K	L	P	L
Gallus gallus D5d	P	S	L	M	H	K	L	P	H
Homo sapiens D5d	P	S	M	M	H	I	L	P	F
Rattus norvegicus D5d	P	S	M	M	H	V	L	P	F

Figure 9. Comparison of the amino acid residues involved in the substrate specificity of rat D6d with corresponding residues in desaturases from various vertebrates. Amino acid residues identical to those in rat D6d (top row) and D5d (bottom row) are indicated with white and black backgrounds, respectively, and other amino acid residues are shown with a gray background.

It is reasonable to assume that the substrate specificity and positioning are determined by the electric charge and polarity of the particular desaturase amino acids, which affect their affinity to the acyl chain and carrier portion of the substrate, and by the depth and angle of

substrate insertion into the binding pocket (46). To evaluate the above-mentioned results of the protein engineering analysis, homology modeling of D6d was carried out on the basis of the recently reported crystal structure of human SCD1 (Protein Data Bank ID 4YMK) (48), using the structure prediction program Phyre2 (57). Amino acid residues of R216, W244, and Q245, located near the substrate-binding pocket (Fig. 10A), are considered to form hydrogen bonds with the pantothenic-acid portion and the carbonyl group of acyl-CoA substrate, according to the findings for SCD1. Substitution of these amino acids with the corresponding D5d residues (M, V, and L, respectively) that do not form hydrogen bonds might alter the substrate-binding strength (Fig. 10B). Simultaneously, the substitutions R216M and W244V seem to cancel the steric hindrance just around the threshold of the pocket, allowing the substrate acyl chain to be inserted much deeper, resulting in the introduction of a carbon–carbon bond at the Δ5 position close to the catalytic site. L323 was predicted to be situated at the bottom of the substrate-binding pocket. The mutation L323F, which conferred Δ5/6 bifunctionality to D6d but might not alter the position of catalytic site nor deform the threshold of the pocket, would strengthen the hydrophobic affinity with the methyl terminus of the substrate acyl chain and/or create more space for insertion of the acyl chain (Fig. 10C).

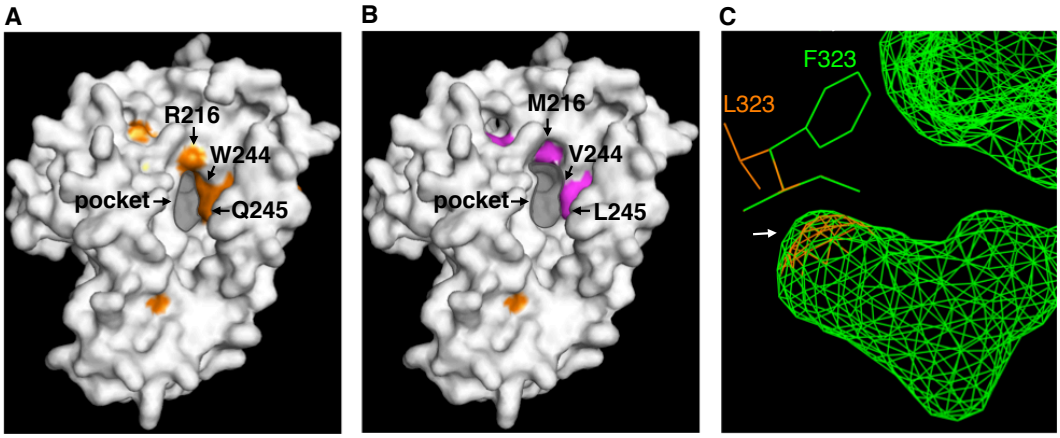

Figure 10. Homology modeling of 3-dimensional structures of rat D6d (A) and the mutants D6d-mut8 (B) and D6d-L323F (C). The models were generated by using the protein structure prediction program Phyre2, with the crystal structure of human stearoyl-CoA desaturase as a template. Amino acid residues that were identified as determinants for substrate specificity and that are located around the entrance of the substrate-binding pocket are indicated by arrows. Panel C compares the predicted structures of the bottom of the internal substrate-binding cavity (an arrow) and the vicinal amino acid residues of intact D6d (orange) and D6d-L323F (green).

2.4 Discussion

On the basis of the structural similarity of the enzymes, the desaturase family is also considered to include hydroxylase that produces hydroxyl fatty acids such as plant surface coating wax (58), conjugase that produces conjugated fatty acids with anti-carcinogenesis activity (59), and acetylenase and epoxidase that produce fatty acids with a triple bond (60) and an epoxy group (61), respectively. Elucidation of the molecular basis of substrate recognition and regio- and chemoselectivity of the enzymes enables us to design new bioactive lipids and to produce them efficiently. In this study, rat D6d and D5d with highly homologous primary structures were used as a model to identify the sites critical for their mutually exclusive substrate specificity.

Heterologous expression analysis of chimeric enzymes of D6d and D5d, in which the cytochrome b_5-like domains were swapped, demonstrated that these domains do not contribute to substrate recognition (Table 2). However, the D6d activity of the chimera D5cyt-D6des was significantly lower than that of intact D6d, suggesting that the cytochrome b_5-like domain might be necessary for full activity of D6d, but not D5d. Therefore, a D6d mutant with D5d activity (equivalent to D6cyt-D5des) would be preferable over the reverse to detect declined desaturase activity. Indeed, the D6d-based mutant D6d-mut8 barely showed D5d activity (Fig. 6B), whereas the introduction of mutations at the corresponding sites in D5d did not result in the generation of detectable D6d product (data not shown). Moreover, given that the distance from the carboxyl group of the fatty acid substrate to the position to be desaturated is considered to be larger in D6d than in D5d, the substrate range of D5d is expected to be wider than that of D6d (62). Thus, site-directed mutagenesis was applied to the D6d gene to readily observe successful conversion of substrate specificity.

I assumed that structural differences between D6d and D5d due to some of the 67 non-conserved amino acids in their hydrophilic regions (Fig. 3) would confer altered substrate specificity. To my knowledge, this study is the first to identify specific positions that are involved in alteration of the substrate selectivity of a mammalian front-end fatty acid desaturase. On the basis of heterologous expression analyses of a series of D6d mutants, I identified 8 mutations (S209P, N211S, R216M, S235M, L236Δ, W244V, Q245L, and V344P) that abolished D6d activity from D6d but conferred D5d activity (Fig. 6B). It is obvious that several amino acid residues are necessary to determine the substrate specificity as well as to support maximum enzymatic activity. The K218 residue of *Mucor rouxii* D6d has been reported to be involved in binding of the substrate (40); however, mutation of the corresponding amino acid in rat, R216, did not yield D5d activity (data not shown). Compared with the D6d-Z2 mutant carrying 12 mutations and with D5d activity 4.6% that of the wild-type D5d (Fig. 5), the D6d-mut8 mutant carrying 8 mutations showed much lower activity (1.4%; Fig. 6B), and the D5d product was not detected in the double mutant R216M/W244V (data not shown). The fact that all of the restored mutants shown in Fig. 6A retained D5d activity suggested that more than 2 critical amino acid residues exist in each group of mutations introduced with the primers d6d5-7/8/10/11 and d6d5-13/21.

The mammalian D6d and D5d and zebrafish bifunctional zD5/6d might have evolved from a common ancestor enzyme (55). Site-directed mutagenesis targeting the residues identical between D5d and zD5/6d but not D6d resulted in the generation of a mutant D6d-25m possessing bifunctional activity (Table 3), and pinpointed L323F as responsible for providing D5d activity to D6d (Fig. 8). However, the mutation L323F was overlooked in the first mutagenesis experiment based on the sequence comparison of only D5d and D6d and the use of multimutagenic primers. This might be because the D5d activity of the D6d-L323F mutant was below the detection limit and/or the other amino acid mutations introduced by the primer (d6d5-18; V321C+F322L+L323F) counteracted its effect. By using two different approaches in

the mutagenesis experiments, a broad-horizon search was achieved, resulting in the determination of the amino acid residues responsible for both switching and adding the substrate specificity of D6d.

In addition, the predicted D6d tertiary structure supported my findings at least in part on the molecular basis of substrate specificity of the fatty acid desaturases. This knowledge will largely contribute to furthering our understanding of the structure–function relationship and the molecular evolution of the desaturase family and to generating structurally and functionally novel fatty acyl compounds for industrial applications.

3. Detection of acyl-CoA derivatized with butylamide for *in vitro* fatty acid desaturase assay

3.1. Introduction

Unsaturated fatty acids are generated through desaturation and elongation of the carbon chain backbone of fatty acid substrates (63). Various types of fatty acid desaturases with different substrate specificities and regioselectivities are found both in prokaryotes and eukaryotes (14, 27, 64). The molecular structure and enzyme characteristics of water-soluble desaturases from cyanobacteria and higher plants, acting on fatty acids bound to acyl carrier protein, have been thoroughly elucidated (29). Besides, the enzymatic activity of membrane-bound desaturases from fungi, algae, plants, and animals that recognize fatty acids bound to coenzyme A (CoA), or associated with glycerides, is determined *in vitro*, most commonly by using microsome fractions prepared from cells or tissues, and radiolabeled substrate (65, 66). However, these assays often involve intricate experimental setup.

Cloned membrane-bound desaturases have been characterized *in vivo* by gene disruption (67, 68), and/or heterologous expression analysis in bacteria, fungi, and higher plants (69–71). The budding yeast, *Saccharomyces cerevisiae*, predominantly contains saturated and mono-unsaturated fatty acids with 16 and 18 carbon atoms (72). This is advantageous since exogenous fatty acid substrates and products can be clearly discriminated from the endogenous fatty acids (73, 74). For instance, Δ6 fatty acid desaturase (D6d) from rat liver has been expressed, identified, and characterized using the yeast expression system, where linoleic acid (LA, 18:2 Δ9, 12) and α-linolenic acid (18:3 Δ9, 12, 15) were converted into GLA (18:3 Δ6, 9, 12) and stearidonic acid (18:4 Δ6, 9, 12, 15) respectively (13), none of which were present endogenously. However, *in vivo* assays cannot precisely determine the chemical kinetics as the amount of enzyme expressed and the amount of substrate incorporated cannot be measured accurately.

In this study, an *in vitro* desaturase reaction was carried out using cell homogenate

from yeast overexpressing D6d and unlabeled acyl-CoA. After specific butylamidation of the acyl-CoA product, acyl butylamide was detected by gas chromatography. This method could serve as a non-radioactive assay for fatty acid desaturase from different sources.

3.2. Experimental procedures

3.2.1. Microorganisms, culture media, and reagents

Transformants of *Escherichia coli* DH5α were selected and cultivated in LB medium (0.5% yeast extract, 1% NaCl, 1% Bacto tryptone, 2% agar for plate) containing 50 μg/mL ampicillin at 37°C with rotary shaking at 120 rpm. Transformants of *S. cerevisiae,* INVSc1 (Invitrogen, Carlsbad, CA, USA) were selected on SD without Ura agar medium (0.67% yeast nitrogen base, 0.19% yeast synthetic dropout medium without uracil, 2% D-glucose, 2% agar) and cultivated in SCT without Ura medium (0.67% yeast nitrogen base, 0.19% yeast synthetic dropout medium without uracil, 4% raffinose, 0.1% tergitol) or YPD medium (2% polypeptone, 1% yeast extract, 2% D-glucose) at 28°C, with rotary shaking at 160 rpm. Fatty acids were purchased from Sigma-Aldrich (St. Louis, MO, USA) or Cayman Chemical (Ann Arbor, MI, USA). Other guaranteed reagents were obtained from Nacalai Tesque (Kyoto, Japan), Sigma-Aldrich, Toyobo (Osaka, Japan), or Wako Chemicals (Osaka, Japan), unless otherwise indicated.

3.2.2. Expression of rat D6d gene in yeast

A FLAG DNA fragment was synthesized by PCR amplification with the TaKaRa Ex Taq (Takara, Kyoto, Japan) and oligonucleotide primers (5'-GCAAAGCTTAAGATGG A*CTATAAGGATGATGATGAC*-3' and 5'-CGTGGTACCCTT*GTCATCATCATCCTTATAG*-3', where these primers can hybridize with each other at nucleotide regions indicated using italics, and underlined regions are *Hin*d III and *Kpn* I recognition sites respectively) using 10 cycles of 95°C for 30 s, 50°C for 30 s, and 74°C for 30 s without template. The fragment was subcloned in the pGEM-T Easy vector (Promega, Madison, WI, USA) and transformed into *E. coli* DH5α (pGEM-FLAG). The rat D6d gene (DDBJ accession number AB021980) (13) was amplified from stock plasmid with the KOD-Dash DNA polymerase (Toyobo) and primers (5'-ACAGGTACC*ATG*GGGAAGGGAGGTAACCAG-3' and 5'-GTCTCTAGAT*TCA*TTTGT

GGAGGTAGGCATCC-3', where underlined regions are *Kpn* I and *Xba* I recognition sites, and italicized regions are translation initiation and termination codons respectively), using 30 cycles of 95°C for 30 s, 68°C for 2 s and 74°C for 30 s, and was digested with *Kpn* I and *Xba* I. The product was ligated into *Kpn* I/*Spe* I-digested pGEM-FLAG and the plasmid was transformed into *E. coli* DH5α (pGEM-FLAG-D6d). The FLAG-D6d fragment was obtained by digestion of pGEM-FLAG-D6d with *Hin*d III and *Eco*R I and was ligated into the yeast expression vector pYES2 (Invitrogen). The nucleotide sequences of all plasmids were determined using BigDye Terminator v3.1 cycle sequencing kit (Life Technologies, Carlsbad, CA, USA) with T7, SP6, and other appropriate primers on an ABI PRISM 3130x1 genetic analyzer (Life Technologies). The desaturase expression vector was introduced into *S. cerevisiae* INVSc1 by using the lithium acetate method (49). Transformants were selected on SD without Ura agar plates and cultivated at 28°C for 12 h with rotary shaking at 160 rpm in 3 mL of SCT without Ura medium. One milliliter of this preculture was transferred to 15 mL of SCT without Ura medium supplemented with linoleic acid (LA) at a concentration of 0.25 mM and cultivated at 28°C for 6 h. After addition of galactose (2%, w/v) and further cultivation for another 16 h, yeast cells were harvested by centrifugation.

3.2.3. *In vitro* desaturase reaction

The yeast cells from 1 mL of induced culture were washed with distilled water and suspended at OD_{600} = 100 in 50 mM Tris-HCl (pH 7.5) containing 1 mM 4-(2-aminoethyl) benzenesulfonyl fluoride hydrochloride and 4.7 μM pepstatin A. Glass beads (particle size of 0.5 mm) were added to the suspension in the same volume, and the yeast cells were disrupted by eight rounds of vigorous vortex for 30 s and chilling on ice for 30 s. The homogenate was centrifuged at 5,000 × *g* for 10 min and the resultant supernatant was centrifuged further at 100,000 × *g* for 1 h at 4°C to obtain the microsomal fraction as precipitate. Protein concentrations of the homogenate and the microsomes were measured by using the BCA protein

assay reagent (Thermo Scientific Fermentas, Carlsbad, CA, USA) (75). The reaction mixture for the *in vitro* desaturation was composed of 50 mM potassium phosphate (pH 7.5), 2 mM NADH, 0.1 mM linoleoyl-CoA, and 2 mg-protein/mL homogenate or microsomes. After incubating the mixture at 30°C for 30 min with reciprocal shaking at 150 rpm, hexane (final concentration of 50%), acetate (1 mM), and *n*-butylamine (2 M) were added to derivatize acyl-CoA by condensing with butylamide (76). The reaction was terminated by the addition of an equal amount of 4 M HCl followed by 2 mL of ethyl acetate and was centrifuged at 2,000 × *g* for 10 min. The fatty acid butylamide contained in the ethyl acetate phase was recovered, transferred to a new tube, evaporated under N_2 airflow, and dissolved with hexane.

3.2.4. Fatty acid analyses

Fatty acid butylamide was analyzed using a gas chromatograph system (GC-2014, Shimadzu, Kyoto, Japan) equipped with a non-polar capillary column (DB-5HT, 0.25 mm × 15 m, Agilent Technology, Santa Clara, CA, USA) under a temperature shift from 100°C to 300°C at 0.5°C/min. γ-Linolenoyl-CoA standard was synthesized by incubating a mixture [40 mM potassium phosphate (pH 7.5), 1 mM ATP, 1 mM $MgCl_2$, 0.2 mM GLA, 1 mM CoA, 0.0025 units/mL acyl-CoA synthetase (Sigma-Aldrich)] at 37°C for 1 h. The mixture was applied to a silica gel column and, after washing the column with hexane/diethyl ether/acetic acid (3:7:0.1, v/v) to eliminate unreacted γ-linolenic acid, γ-linolenoyl-CoA was eluted with butanol/water/acetic acid (5:3:2, v/v) and derivatized with butylamide as mentioned above to be used as a standard in the gas chromatography analysis.

To analyze fatty acid methyl esters, the yeast cells from 15 mL of culture broth were washed with distilled water and vigorously vortexed in 2 mL of chloroform/methanol (2:1, v/v) plus 0.5 mL of distilled water. The chloroform phase was recovered by centrifugation and methanolysis of total lipid was performed by adding 1 mL of 10% methanolic hydrochloric acid (Tokyo Kasei, Tokyo, Japan) followed by heating at 60°C for 2 h. After evaporation of the

solvents, fatty acid methyl esters (FAMEs) were extracted twice and dissolved in hexane. Fatty acid composition was determined using gas chromatographic system equipped with a capillary column (TC-70, 0.25 mm × 30 m, GL Sciences, Tokyo, Japan). FAMEs were identified by comparing their retention time with those of the 37-Component FAME mix (Supelco, Bellefonte, PA, USA). The enzymatic activity of the desaturase expressed in yeast was evaluated using the conversion ratio, which was determined as the ratio of the amount of product to the sum of the amounts of substrate and product and was expressed as a percentage.

3.2.5. SDS-PAGE and western blotting

The yeast cell homogenate prepared as mentioned in the section 3.2.3. was centrifuged at 5000 × *g* for 10 min and the supernatant was subjected to SDS-PAGE (50). Proteins separated in the gel were transferred to an Immobilon membrane (Merck Millipore, Darmstadt, Germany) using a semi-dry blotter. The membrane was blocked by immersing in 5% skim milk in PBST (137 mM NaCl, 2.7 mM KCl, 10 mM Na_2HPO_4, 1.76 mM KH_2PO_4, 0.05% (w/v) Tween-20), and then moved to the same buffer containing mouse anti-FLAG antibody (Sigma-Aldrich; 1:10000). After shaking for 1 h and washing with PBST, the membrane was probed with rabbit anti-mouse IgG (1:20000) for 1 h. The FLAG-tagged proteins were detected by using ECL select (GE Healthcare, Buckinghamshire, UK) and exposure to LAS-500 (GE Healthcare, Buckinghamshire, UK).

3.3. Results

3.3.1. Functional expression of FLAG-D6d in yeast

The D6d gene tagged with a FLAG peptide at the N-terminal was expressed in *S. cerevisiae* INVSc-1 in the presence of LA, and the intracellular fatty acid composition was determined. As shown in Fig. 11A, GLA, as the Δ6 desaturation product from LA, was generated at the conversion rate of 23.1%. It was not detected at all in the control experiment using an empty vector. The western blotting analysis using anti-FLAG antibody could detect the production of the 52-kDa FLAG-D6d protein, only when the D6d gene was expressed (Fig. 11B). Therefore, the active D6d with a FLAG tag was successfully expressed in yeast.

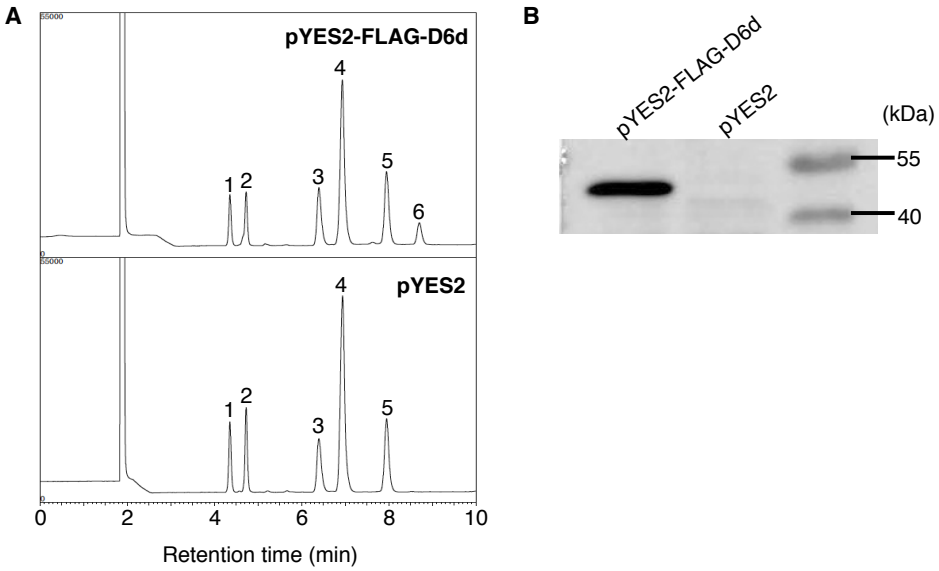

Figure 11. Expression of active FLAG-D6d in yeast *S. cerevisiae* containing an expression vector, pYES2-FLAG-D6d or pYES2, was cultivated in SCT medium and induced by the addition of galactose. A: Gas chromatograms of fatty acid methyl esters from total lipids in the induced yeast cells. Peak 1, 16:0; 2, 16:1; 3, 18:0; 4, 18:1 Δ9; 5, exogenously added 18:2 Δ9,12; 6, product 18:3 Δ6,9,12. B: Western blot analysis. Total proteins were separated by SDS-PAGE and transferred to a membrane. The FLAG-D6d was detected with anti-FLAG antibody as described in Experimental procedures.

3.3.2. Timing of expression of maximum D6d activity

In the yeast system, the expression of the D6d gene, under the control of Gal1 promoter was stably induced by the addition of galactose. However, the time required to reach the maximum activity of D6d had not been determined. During the cultivation of

D6d-expressing yeast cells in the presence of galactose, the substrate, LA, was added at various time points. Two hours after each addition, yeast cells were harvested and their fatty acid composition was measured. The maximum rate of conversion from LA to GLA (25.9%) was observed when LA was added 4-6 hours after induction, as seen in Fig. 12. Thus, 4 h after the gene induction was identified as the best time to obtain the maximum D6d activity, and was used to harvest the yeast cells for *in vitro* reaction.

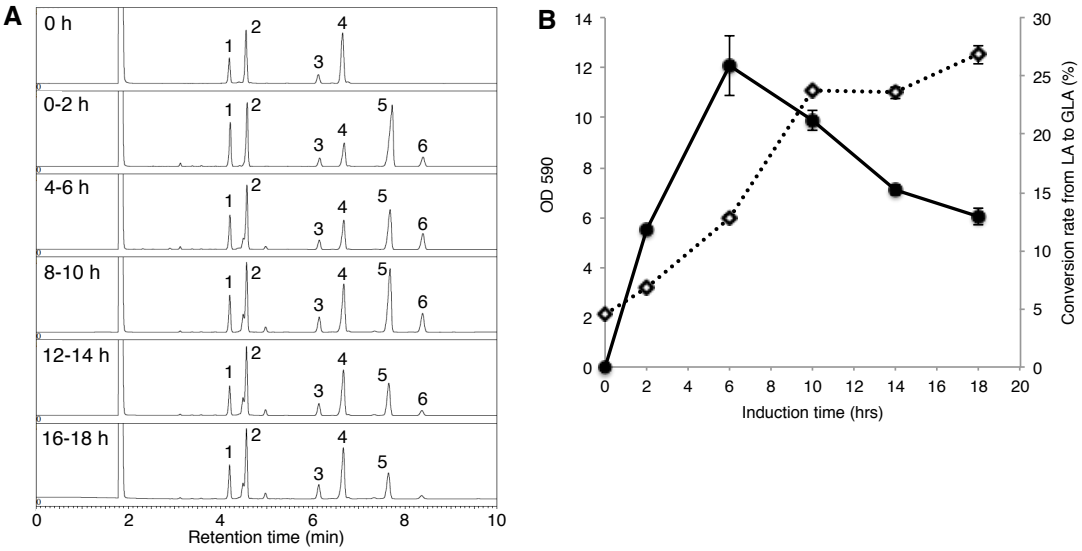

Figure 12. Time-course of *in vivo* D6d activity in *S. cerevisiae*. The expression of D6d gene was induced by the addition of galactose to the culture medium at 0 h. and LA was added at 0, 4, 8, 12, or 16 h after the induction. The yeast cells were harvested 2 h after the addition of substrate and fatty acid composition in total lipid was analyzed. A: Gas chromatograms of fatty acid methyl esters from total lipids of the D6d-expressed yeast cells harvested just before the addition of substrate (0 h) or at the end of each reaction period (2, 6, 10, 14, or 18 h). Peak numbers are the same as in Fig. 11. B: Yeast cell growth (OD; open diamonds) and D6d activity (filled circles). The D6d activity was indicated as conversion rate of LA to GLA 2 h after the addition of substrate.

3.3.3. *In vitro* D6d reaction using yeast cell homogenate and microsomes

The D6d-expressing yeast cells were mechanically disrupted, and the microsome fraction was prepared from the homogenate to detect the successful expression of the FLAG-D6d by western blotting as shown in Fig. 13A. The homogenate and microsomes containing the D6d protein were used for *in vitro* desaturase reaction with the substrate, linoleoyl-CoA. Fig. 13B shows the gas chromatograms of the butylamide derivatives of the

product with the same retention time as γ-linolenoyl butylamide generated in the reaction mixture using the cell homogenate. This result demonstrated the usefulness of the proposed method for *in vitro* desaturation assay. However, this compound was not detected when no substrate was added to the reaction or microsomes were used instead of the homogenate (data not shown).

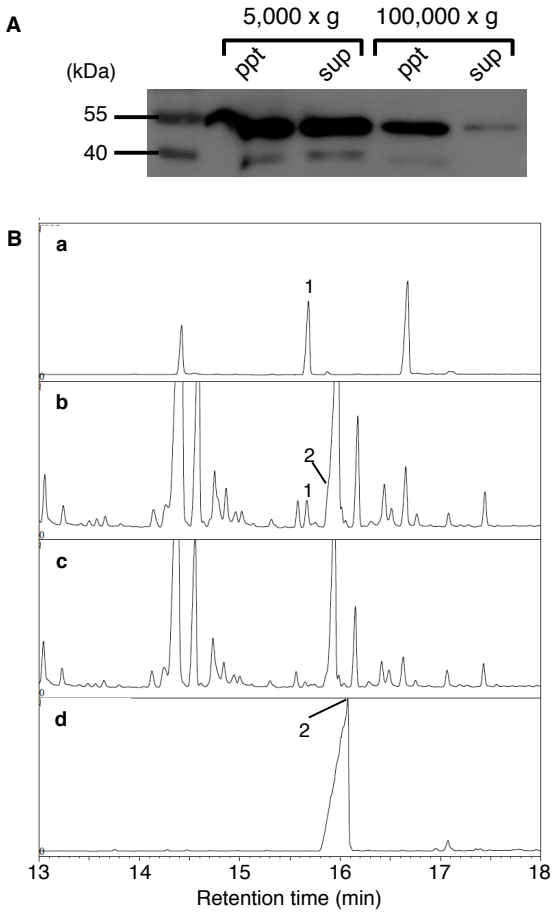

Figure 13. *In vitro* desaturase reaction by homogenate or microsomes prepared from D6d-expressing yeast cells with linoleoyl-CoA. A: Disrupted yeast cells were centrifuged at 5000 × g and the resultant supernatant (sup) was ultracentrifuged at 100,000 × g to recover the microsomes (ppt). The FLAG-D6d was detected by western blotting using anti-FLAG antibody. B: *In vitro* desaturation reaction by cell homogenate with linoleoyl-CoA (panel b). After the reaction for 30 min, acyl-CoAs were derivatized with *n*-butylamine and analyzed by gas chromatography. The D6d product was identified by comparing the retention time with that of γ-linolenoyl butylamide (peak 1, panel a) derivatized from γ-linolenoyl-CoA, synthesized as described in Experimental procedures. Panel a: γ-linolenoyl butylamide standard; c: reaction mixture without linoleoyl-CoA; d: reaction mixture without cell homogenate. Peak 1: γ-linolenoyl butylamide; 2: linoleoyl butylamide. Other peaks in panel a: residual TritonX-100.

3.4. Discussion

Previously reported *in vitro* desaturase reactions, using microsomes as an enzyme fraction and acyl-CoA as a substrate, had to perform saponification and methylesterification of acyl-CoA products to detect them by gas chromatography (65, 66). Since fatty acids contained in glycerolipids and glycolipids in the membrane fractions are methylesterified as well, the reaction product could not be discriminated from endogenous compounds. The use of radio- and stable isotopes of fatty acid substrate requires a restricted area and exclusive facilities, and is often not quantitative in nature. In this study, non-labeled acyl-CoA was used as a substrate, the reaction product was derivatized with butylamide (76), and detected by gas chromatography (Fig. 13B). To the best of my knowledge, this is the first attempt to detect the *in vitro* desaturation product using non-labeled acyl-CoA as the substrate. Since butylamine reacts only with fatty acid thioesters, but not with esters without thiol, this approach distinguishes fatty acids generated by the desaturation reaction from the endogenous species. The butylamidation treatment after the purification of the generated acyl-CoA (76), if necessary, will diminish the disturbances in the background and fulfill the criteria for quantitative measurement. Moreover, the substrate, acyl-CoA, can be obtained from manufacturers or synthesized by users themselves through chemical procedures (77), and enzymatic methods that have been applied to prepare γ-linolenoyl-CoA in this study. Therefore, any species of fatty acid can be used as a substrate.

In *in vitro* desaturation reaction using membrane fractions from animal tissues (65) and plant plastids (66), the fatty acid substrate and product may be consumed or modified by intrinsic metabolic systems. This might be the case even in the yeast heterologous expression system like the one used in this study as only the cumulative total of the generated product has been measured. Therefore, it would be more precise to determine the change of substrate and product concentrations with the lapse of time during the reaction. Here, I have investigated the time to obtain the maximum D6d activity after the induction of gene expression and determined that 4 h post induction was the best time to harvest the yeast cells for use in *in vitro* reaction.

The appropriate timing should be set for each instance of the experiment.

Since the mammalian membrane-bound type desaturases are known to associate with endoplasmic reticulum (78), the D6d activity was expected to be concentrated in the microsome fraction. Indeed, the D6d protein was detected in the precipitates after ultracentrifugation but the generation of γ-linolenoyl-CoA was not observed in *in vitro* reaction with the microsomes (data not shown). In *in vitro* desaturation reactions using microsomes prepared from rat liver or flax seeds, the addition of supernatant obtained after the ultracentrifugation, or the supplementation of purified catalase was effective in boosting the desaturase activity (79, 80). The identification of such a specific component that results in maximum activity will be critical in standardizing the *in vitro* desaturase reaction.

4. Purification of mammalian front-end fatty acid desaturases.

4.1. Introduction

Δ6 desaturase and Δ5 desaturase (D6d and D5d) (13, 27) belong to front-end desaturases (36) that introduce new double bonds between the preexisting double bond and the carboxyl end of fatty acid. They are responsible for the production of polyunsaturated fatty acid (PUFA) which are valuable as medicine and health supplement (63). Fatty acid desaturation is an oxidation-reduction reaction that requires NADH (81) and cytochrome b_5 as electron transport factors (82). Front-end desaturases have cytochrome b_5-like domain in the N-terminal regions of enzymes in common. Previously, we elucidated that both of this domain and diffused cytochrome b_5 in endoplasmic reticulum were necessary for expression of maximum activity of rat D6d (28), but the exact molecular mechanism was unrevealed. Although elucidation of molecular mechanism of electron transportation between the cytochrome b_5-like domain and the active center of desaturation will contribute to the improvement of the reaction efficiency of these enzymes, homology modeling cannot be applied because of the lack of cytochrome b_5-like domain in stearoyl CoA desaturase (SCD1) (22, 23). Therefore, structural biology the approach to cytochrome b_5 reductase fusion desaturase is necessary in order to elucidate the electron transport mechanism of this domain. Thus, in this chapter, I attempted to construct the production system of purified cytochrome b_5 fusion desaturase, which is necessary for crystal structure analysis of this enzyme.

4.2. Experimental procedures

4.2.1. Microorganisms, culture media and regents

LB medium (0.5% yeast extract, 1% NaCl, 1% Bacto tryptone, 2% agar for plate) containing 50 μg/mL ampicillin was used for selection of transformants of *Escherichia coli* DH5α at 37°C with rotary shaking at 120 rpm. Transformants of *Pichia pastoris* GS115 (Invitrogen, Carlsbad, CA, USA) were selected on MD agar medium (1.34% yeast nitrogen base, 2% D-glucose, 0.04 ppm biotin, 2% agar) and cultivated in MGY medium (1.34% yeast nitrogen base, 1% glycerol, 0.04 ppm biotin), MM medium (1.34% yeast nitrogen base, 0.5% methanol, 0.04 ppm biotin) or YPG medium (2% polypeptone, 1% yeast extract, 1% glycerol). Fatty acids were purchased from Sigma-Aldrich (St. Louis, MO, USA) or Cayman Chemical (Ann Arbor, MI, USA). Restriction enzymes were purchased from Takara (Osaka, Japan) or New England Biolabs (Ipswich, MA, USA). Detergents for solubilization of desaturases were purchased from Dojindo Molecular Technology (Kumamoto, Japan) and Nacalai Tesque (Kyoto, Japan). Other guaranteed reagents were purchased from Nacalai Tesque, Sigma-Aldrich, Toyobo (Osaka, Japan), or Wako Chemicals (Osaka, Japan), unless otherwise indicated.

4.2.2. Construction of plasmid for desaturase expression

The FLAG-tagged rat D6d gene (DDBJ accession number AB021980) was obtained by digestion of stock plasmid with *Eco*R I and was ligated into the *P. pastoris* expression vector pPIC3.5K (Invitrogen) (pPFLAG-d6). The FLAG-tagged rat D5d gene was amplified from stock plasmid with Ex-Taq DNA polymerase (Takara, Kyoto, Japan) and primers (5'-GCAAGATCTAAG*ATG*GACTATAAGGATGATGATGAC-3' and 5'-TCAGCGGCCGC *CTA*TTGGTGAAGGTAAGCATC-3', where underlined regions are *Bgl* II and *Not* I recognition sites, and italicized regions are translation initiation and termination codons respectively), using 30 cycles of 94°C for 30 s, 60°C for 30 s and 72°C for 60 s, and was digested with *Bgl* II and *Not* I. The product was ligated into *Bgl* II/*Not* I-digested pPIC3.5K

(pPFLAG-d5) and the constructed plasmids were transformed into *E. coli* DH5α. The nucleotide sequences of all plasmids were determined using BigDye Terminator v3.1 cycle sequencing kit (Life Technologies, Carlsbad, CA, USA) with primers (5'-GACTGGTTCCAATTGACAA GC-3', 5'-GCAAATGGCATTCTGACATCC-3', 5'-AAAACCAACCACCTGTTCTTCT-3', 5'-GAATCCAGCCATTGCCGAAGTA-3', 5'-TGCTCATCCCTATGTACTTCCA-3 and 5'-G GATATAGGTGTAGAAGAAACG-3') on an ABI PRISM 3130x1 genetic analyzer (Life Technologies).

4.2.3. Western blot analysis

The yeast cells collected from 1 ml culture broth were suspended at OD_{600}=100 in 50 mM Tris-HCl (pH 7.5) containing 1 mM 4-(2-aminoethyl) benzenesulfonyl fluoride hydrochloride and 4.7 μM pepstatin A. Cell disruption was performed by addition of glass beads (particle size 0.5 mm) and eight rounds of vortex for 30 s and incubation on ice 30 s. Debris were removed by centrifugation at 5,000 × g, for 10 min, and supernatant were used for SDS-PAGE (50). Extracted proteins were separated by 12.5% polyacrylamide gel and transferred to Immobilon membrane (Merck Millipore, Darmstadt, Germany) using semi-dry blotter. The membranes were blocked with 5% skim milk in PBST (137 mM NaCl, 2.7 mM KCl, 10 mM Na_2HPO_4, 1.76 mM KH_2PO_4, 0.05% (w/v) Tween-20) overnight at 4ºC. The blocked membranes were rinsed with PBST buffer, and incubated with mouse anti-FLAG antibody (Sigma-Aldrich) diluted 1: 10000 with PBST for 1 h. After washing with PBST, the membranes were incubated in PBST containing rabbit anti-mouse IgG-HRP (Sigma-Aldrich) diluted 1:20000 for 1 h. The FLAG-tagged desaturases were detected by using ECL select (GE Healthcare, Buckinghamshire, UK) and LAS-500 (GE Healthcare).

4.2.4. Fatty acid analysis

The yeast cells from 15 ml culture were washed with distilled water, and total lipid

was extracted with Folch method (83). Fatty acid methylesters (FAMEs) for analysis were prepared by addition of 1 ml of 10% methanolic hydrochloric acid (Tokyo Kasei, Tokyo, Japan) to total lipid from yeast and heating at 60ºC for 2 h. The solvent was evaporated under the nitrogen stream, and FAMEs were extracted with hexane. FAMEs dissolved in 100 µl hexane were used in analysis. FAMEs content was determined using gas chromatographic system with flame ionization detector and capillary column (TC-70, 0.25 mm × 30 m, GL Sciences, Tokyo, Japan). 37-Component FAME mix (Supelco, Bellefonte, PA, USA) was used for identification of FAMEs from yeast. The enzymatic activity of each desaturase in yeast was estimated using substrate conversion rate (the ratio of the amount of product to the sum of the amounts of substrate and product).

4.2.5. Expression of desaturase genes in *P. pastoris*

pPFLAG-d6 and pPFLAG-d5 were linearized with *Sal* I and *Sac* II, respectively. The desaturase expression vectors were introduced into *P. pastoris* GS115 by the electroporation method (84). Transformants were selected on MD agar plates. The colonies of transformants on MD agar plate were suspended into sterilized water and plated (10^5 cells) on YPD agar plate containing 4 mg/ml G418（Sigma Aldrich）and incubated at 30ºC for selection of transformants containing multiple insert in their genome. G418-resistant strains were cultivated in 3 mL of MGY medium at 28°C for 24 h with rotary shaking at 160 rpm. The yeast cells collected from the preculture were washed with sterilized water and suspended at OD_{600} = 1.0 in MM medium. MM medium with exogenous dihomo-γ-linolenic acid (DGLA) at a concentration of 0.25 mM was used, in the case of cultivation of D5d expression yeast. Transformants were cultivated at 28ºC for 48 h with rotary shaking at 250 rpm, and methanol (0.25%, v/v) was added every 12 h from the initiation of culture for the induction of desaturase expression.

4.2.6. Large scale cultivation using jar fermenter

P. pastoris cells collected from preculture were washed with sterilized water and suspended at OD_{600} = 1.0 in 7 L-MM medium in jar fermenter (10 L capacity) and cultivated for 48 h at 30ºC, 10 L /min of air supply with stirring at 300 rpm. Methanol (0.25%, v/v) was added every 12 h for the expression of desaturases. In the case of high-density cultivation using YPG medium as expression medium, preculture was supplied at OD_{600} = 0.2 into YPG medium in jar fermenter and cultivated for 72 h in same conditions described above. Desaturase expression was induced by addition of methanol (0.5%, v/v) at 24, 36, 48 and 60 h after the start of culture.

4.2.7. Solubilization of desaturases by detergents

The yeast cells from 1 L culture were suspended in 50 ml of 50 mM Tris-HCl (pH 7.5) containing 1 mM 4-(2-aminoethyl) benzenesulfonyl fluoride hydrochloride and 4.7 μM pepstatin A. Cells were disrupted in FRENCH Pressure Cells (Thermo Fisher scientific) using 2100 kg/cm^3. The homogenate was centrifuged at 5,000 × g for 10 min and the resultant supernatant was centrifuged further at 100,000 × g for 1 h at 4°C to obtain the microsomal fraction as precipitate. The precipitate was suspended at the concentration of 1 mg/ml-total protein in solubilization buffer containing 50 mM Tris-HCl pH 7.5, 150 mM NaCl, 15% glycerol and each detergent. Detergents; *n*-Dodecylβ-D-maltoside (DDM), Triton X-100, Brij 35 and Tween 20 were used for solubilization of D6d, and DDM, Decyl-maltoside (DM), Octyl-maltoside (OM), Octyl-glucoside (OG), Triton X-100, MEGA-10 and Fos-choline 12 were used for solubilization of D5d. Solubilization of desaturases was performed with gently shaking at 4ºC for 2 h. Solubilized proteins were collected in supernatant by centrifugation at 100,000 × g for 1 h at 4°C. FLAG-tagged desaturases in supernatant and precipitate were detected by western blotting using anti-FLAG antibody. Solubilization efficiency by each detergent was calculated by ratio of the amount of the desaturase in supernatant to the sum of the amounts of desaturases in supernatant and precipitate.

4.2.8. Affinity chromatography

Anti-FLAG M2 affinity gel (Sigma Aldrich) equilibrated by TBS buffer (50 mM Tris-HCl, pH 7.5, 150 mM NaCl, 0.05% DDM) was added to the soluble protein fraction solubilized by 0.1% DDM, and mixed gently for 2 h at room temperature. The affinity gel was collected as precipitate by centrifugation at 1,500 × g, and supernatant was sampled as the pass-through fraction. The affinity gel in the open column was washed with TBS buffer for removing non-specific binding proteins, and elute was sampled as the wash fraction. The FLAG-tagged desaturases were eluted using 2 ml TBS buffer containing 3× FLAG peptide (100 μg/ml) (Sigma Aldrich).

4.2.9. Gel filtration chromatography

3×FLAG peptide included in the elution fraction of affinity chromatography was removed by size fractionation using the Superdex 200 10/300 (10 mm × 300 mm, GE healthcare) and Akta explorer 10S (GE healthcare). The affinity purified D6d sample was passed thorough a column equilibrated with TBS buffer. The elution fractions containing purified D6d were condensed using Amicon Ultra-10 kDa (Amicon).

4.3. Results

4.3.1. Functional expression of FLAG–tagged desaturases by *P. pastoris* GS115

The D6d and D5d genes tagged with FLAG peptide at the N-terminal were introduced into *P. pastoris*, and the expression of each desaturase gene was induced by addition of methanol. The western blotting analysis using anti-FLAG antibody could detect the production of FLAG-D6d (52,380 Da) and FLAG-D5d (53,766 Da) (Fig. 14A). As the result of analysis of intercellular fatty acid composition of yeast expressing FLAG-D6d, γ-linolenic acid (18:3 Δ6,9,12) and stearidonic acid (18:4 Δ6,9,12,15), which are the D6d products, were generated from linoleic acid (18:2 Δ9,12) and α-linolenic acid at the conversion rate of 19.5% and 32.0%, respectively (Fig. 14Bb). In the case of cultivation of D5d expression yeast in MM medium with exogenous dihomo-γ-linolenic acid, arachidonic acid (the product of D5d) was generated at the conversion rate of 19.5% (Fig. 14Cb). Thus, active FLAG-D6d and FLAG-D5d were successfully expressed.

4.3.2. Selection of detergents for solubilization of desaturases

In order to solubilize the D6d and D5d proteins associating with biological membrane, the condition of desaturase solubilization by various detergents were examined. The microsomal fraction containing endoplasmic membrane where desaturases were localized was collected from yeast cell lysate by ultracentrifugation and incubated with each detergent described in Experimental procedure. After incubation, solubilized enzymes and non-solubilized enzymes were separated by ultracentrifugation, and I compared the amount of solubilized desaturases that are recovered in supernatant. Some detergents (0.05% DDM, 0.05% Triton X-100 and 0.5% Brij 35) especially solubilized D6d at the rate of 99%, 95%, and 83%, respectively (Fig. 15A). Meanwhile, 0.05% DDM, 0.1% DM and 0.05% Triton X-100 solubilized more than half of D5d at the rate of 61%, 64% and 83%, respectively (Fig. 15B).

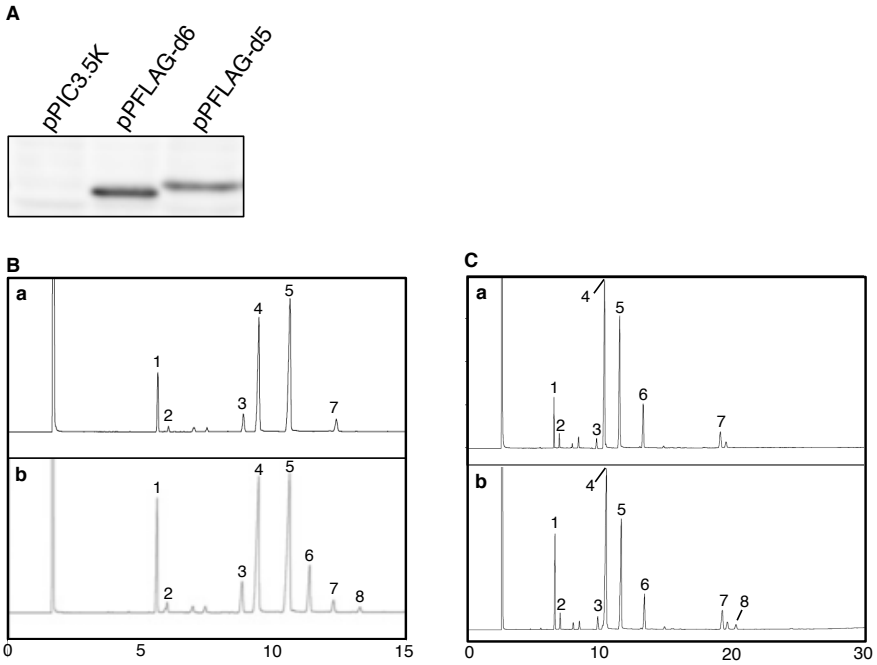

Figure 14. Heterologous expression of FLAG-D6d and FLAG-D5d in *P. pastoris*. A: Western blot analysis. Total proteins from yeast containing an expression vector, pPFLAG-d6, pPFLAG-d5 or pPIC3.5K were separated by SDS-PAGE and transferred to a membrane. The FLAG-tagged D6d and D5d were detected with anti-FLAG antibody as described in Experimental procedures. B: Gas chromatograms of fatty acid methyl esters from total lipids in yeast containing pPFLAG-d6 (b) and pPIC3.5K (a). Peak 1, 16:0; 2, 16:1; 3, 18:0; 4, 18:1 Δ9; 5, 18:2 Δ9,12; 6, product 18:3 Δ6,9,12; 7, 18:3 Δ9,12,15; 8, product 18:4 Δ6,9,12,15. C: Gas chromatograms of fatty acid methyl esters from total lipids in yeast containing pPFLAG-d5 (b) and pPIC3.5K (a). Peaks 1-5 are same with panel B. Other peaks 6, 18:3 Δ9,12,15; 7, exogenously added 20:3 Δ8,11,14; 8, product 20:4 Δ5, 8,11,14.

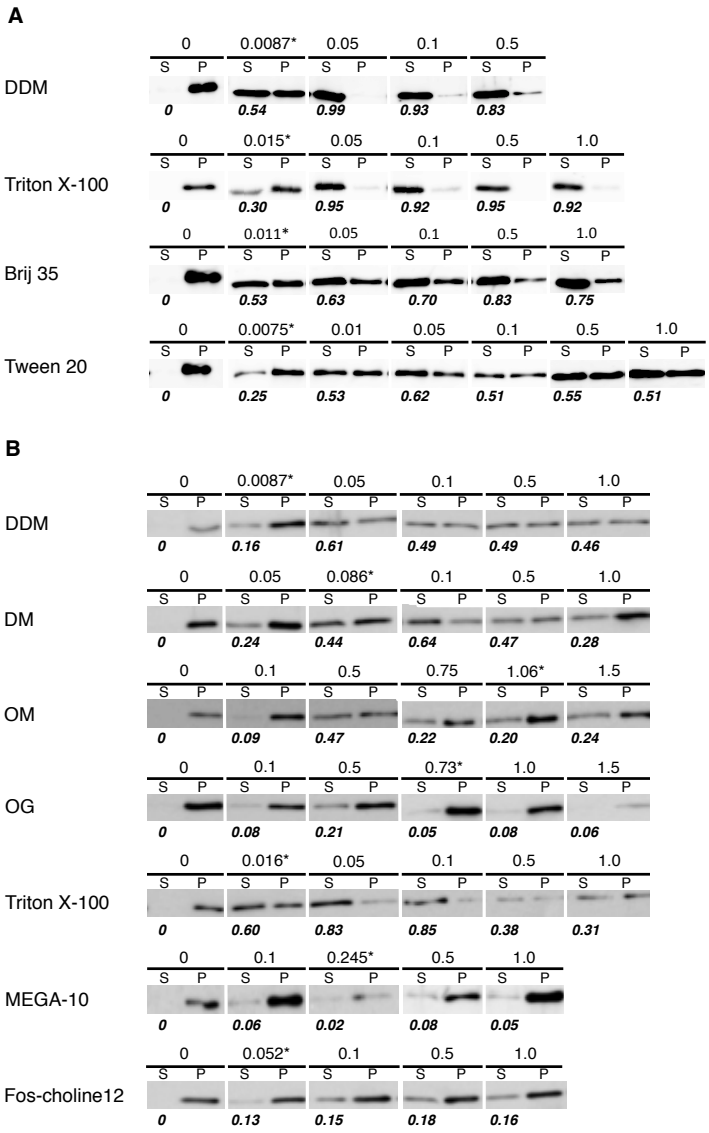

Figure 15. Microsomes harvested from *P. pastoris* were incubated with various concentrations (values above the bands) of detergents. After the ultra-centrifugation, solubilized desaturases were detected in the supernatant (S), and non-solubilized enzymes were detected in the precipitate (P) by western blotting. The solubilization efficiency (italic values under the band) was expressed as enzyme existence ratio in supernatant. (A) *n*-Dodecylβ-D-maltoside (DDM), Triton X-100, Brij 35 and Tween 20 were used for solubilization of D6d. (B) DDM, Decyl-maltoside (DM), Octyl-maltoside (OM), Octyl-glucoside (OG), Triton X-100, MEGA-10 and Fos-choline 12 were used for solubilization of D5d.

4.3.3. Purification of D6d and D5d

FLAG-tagged D6d and D5d solubilized by 0.1% DDM were bound to anti-FLAG M2 affinity gel. Non-specific proteins were washed out with TBS buffer, and FLAG-tagged

desaturases binding to affinity gel were eluted competitively using TBS buffer containing 3×FLAG peptide. As a result, the clear band of D6d was detected in coomassie blue staining (Fig. 16A; lane 8). In order to remove 3×FLAG peptide from the elution fraction of affinity chromatography, the affinity-purified protein was subjected to gel filtration chromatography. As a result, the single band of D6d without low molecular weight band of FLAG peptide was detected in coomassie blue staining (Fig. 16B; lane 3). The D6d yield was estimated as 1.12 mg/L-culture by the comparison of band intensity with molecular weight marker. In the case of affinity chromatography of D5d, the concentration of FLAG-D5d was too low to be detected in coomassie blue staining, whereas the positive band was detected in western blotting using anti-FLAG antibody (Fig. 16C; lane 10). As the result of condensation of FLAG-D5d by ultrafiltration, the clear band of FLAG-D5d was detected at the position of predicted molecular weight (Fig. 16C; lane 11).

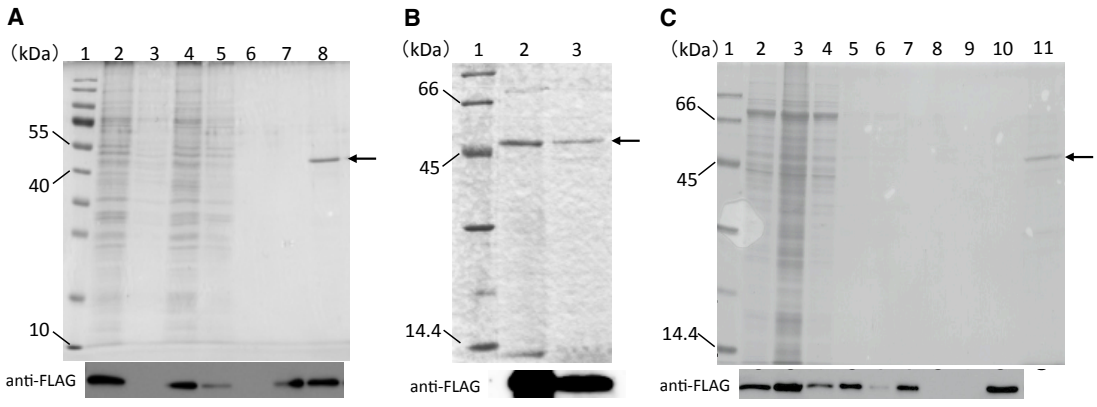

Figure 16. Purification of solubilized desaturases by affinity chromatography and gel filtration chromatography. Existence of FLAG-tagged D6d or D5d in each fraction was detected by coomassie blue staining and western blotting. Solid arrows indicate the bands of desaturases. A: Affinity chromatography of D6d. Lane 1, molecular weight marker; 2, microsomal fraction; 3, non-solubilized proteins; 4, solubilized protein by DDM; 5, pass-through fraction; 6, wash fraction; 7, elution fraction-1; 8, elution fraction-2. B: Gel filtration chromatography of D6d. Lane 1, molecular weight marker; 2, affinity-purified D6d; 3, D6d purified by gel filtration. C: Cell fractionation and affinity chromatography of D5d. Lane 1, molecular weight marker; 2, supernatant of cell lysate; 3, precipitate of cell lysate; 4, supernatant of ultracentrifugation; 5, precipitate of ultracentrifugation (microsomal fraction); 6, solubilized protein by DDM; 7, non-solubilized proteins; 8, pass-through fraction; 9, wash fraction; 10, elution fraction; 11, the concentrate of elution fraction.

4.3.4. Optimization of cultivation condition for improvement of desaturase productivity

In order to improve the productivity of membrane-bound desaturases by *P. pastoris*, YPG medium, which is rich in nitrogen source, was used instead of minimum medium for induction of expression of desaturase genes, and large-scale cultivation using jar fermenter was performed.

The yeast containing pPFLAG-d5 was cultivated in YPG medium, and induction of D5d expression was induced by addition of methanol at 24 h from the initiation of culture. The cell density (OD_{600}) increased 19.5-fold (Fig. 17A) compared with that of cultivation using minimum medium (OD_{600} = 3.1). D5d productivity improved 17.2-fold compared with the cultivation using MM medium on same condition (Fig. 17B). Moreover, the tracking experiment of D5d expression level revealed that D5d production per culture reached stationary at 6 h from the start of induction (Fig. 17B).

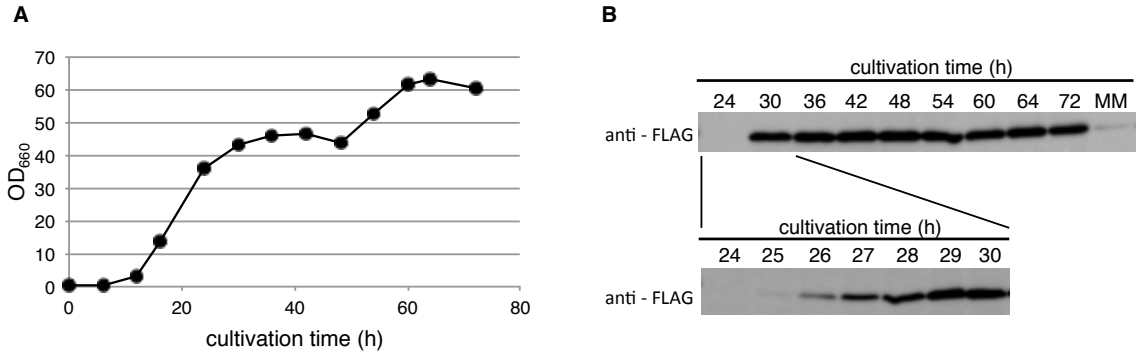

Figure 17. Optimization of culture condition for improving the D5d productivity. *P. pastoris* containing an expression vector pPFALG-d5 was cultivated in 7L YPG medium in jar fermenter. The expression of D5d gene was induced by the addition of methanol to the culture medium at 24 h, and cell density and D5d expression level per culture medium were monitored. A: Yeast cell growth (OD_{660}; filled circle). B: D5d expression level at each timing was quantified by western blotting and compered with in the case of using MM medium on same cultivation condition.

4.4. Discussion

The purified protein production systems were required for the crystal structure analysis of membrane protein. In this section, I constructed the mass production system of Δ6 and Δ5 fatty acid desaturases from *R. norvegicus* using methylotrophic yeast *P. pastoris* and purification system of desaturases. Though the purification of human Δ9 fatty acid desaturase (23, 48, 85) and Δ9, Δ12, Δ15 acyl-lipid desaturases from *Mortierella alpine* (86) were reported, this is the first study about the purification of cytochrome b_5 fusion desaturases as far as I know.

I expected high-level expression of heterologous proteins by incorporating desaturase genes under the alcohol oxidase (AOX) promoter of *P. pastoris*. Indeed, active type FLAG-tagged D6d and D5d were expressed (Fig. 14). Since heterologous genes were inserted into the *Pichia* genome and maintained stably, I used nitrogen-rich medium (YPG medium) instead of minimum medium. Consequently, high cell density cultivation was performed, and the expression level of D5d increased 17.2-fold (Fig. 17B) compared with the case of using MM medium. Furthermore, time course analysis of D5d expression showed that the expression level reached a plateau at 6 h after the induction and this result contributed to shortening of cultivation time (Fig. 17B).

The solubilization of membrane-bound protein without denature of natural conformation by detergent is essential for purification. Since non-ionic detergents were usually used in crystallization of membrane-bound proteins (87, 88), non-ionic detergents except Fos-choline 12 were used for solubilization of D6d and D5d. Considering the effect of detergents on purification step, I examined the necessary and sufficient concentration of detergents in order to solubilize D6d and D5d, respectively. *N*-dodecyl *ß*-maltoside (DDM), Triton X-100 and Brij 35 solubilized 88-99% of D6d (Fig. 15A), and DDM, *n*-decyl *ß*-maltoside (DM) and Triton X-100 solubilized 61-83% of D5d (Fig. 15B). Though detergents which contain sugars as hydrophilic headgroups including DDM and DM were used in solubilization

of acyl-CoA desaturase SCD1 (23, 48), it was indicated that these detergents were also effective in solubilizaton of cytochrome b_5 fusion desaturases.

Since DDM were often used in crystallization of membrane bound enzyme (48, 89, 90), this detergent was used in solubilization of D6d and D5d for purification in this study. As a result of the affinity chromatography with anti-FLAG affinity gel and the gel filtration, solubilized D6d was purified to homogeneity in coomassie blue staining (Fig. 16). Though the D6d yield (1.12 mg/L-culture) was less than reported yields of purified Δ9, Δ12, Δ15 desaturases from *M. alpina* (37.5, 2.5, 4.6 mg/L-culture, respectively) with same expression host (86), further improvement of yield was expected by high cell density cultivation using YPG medium.

In order to confirm that purified D6d still maintained the native structure and activity, I had some trials using purified D6d, linoleoyl-CoA substrate and electron transfer factors such as NADH and cytochrome b_5 reductase. For instance, I carried out the *in vitro* reaction using D6d reconstructed into microsomes prepared from yeast (91), or using solubilized D6d with purified cytochrome b_5 reductase (30). Though D6d activity was not unfortunately detected in both experiments (data not shown), the *in vivo* activity of FLAG-tagged desaturases and the crystal structure of SCD1 purified in the similar manner support that D6d and D5d did not lose the native conformation.

In this section, I constructed the purification system of cytochrome b_5 fusion fatty acid desaturases. This system will become a basis on the crystal structure analysis of desaturase family enzymes and contribute to the elucidation of structural basis of various substrate specificity and regioselectivity.

5. Conclusion

In my thesis, I attempted to elucidate the structure-function relationship of desaturase family enzymes that govern the production of modified fatty acids that exhibit various physiological activities in living body. The findings obtained in my research were described as below.

In chapter 2, I identified eight amino acids (Ser209, Asn211, Arg216, Ser235, Leu236, Trp244, Gln245 and Val344) of D6d as determinants of substrate specificities, and the substitution of these residues with the corresponding residues of D5d switched the substrate specificity. Furthermore, the substitution of Leu323 of D6d with Phe323 on the basis of the amino acid sequence of zebrafish Δ5/6 bifunctional desaturase provided bifunctionality to D6d. The homology modeling with the crystal structure of human Δ9 stearoyl-CoA desaturase revealed the mechanism of expression of D5d activity by mutations. It was suggested that substitutions R216M, W244V and L323F allowed the substrate acyl chain to be inserted much deeper and induced the expression of D5d activity.

In chapter 3, in order to measure the activities of acyl-CoA desaturases including D6d and D5d more exactly, I constructed the *in vitro* reaction and detection method that is more quantitative and simpler compared to conventional methods. The homogenate prepared from D6d expressing yeast was made to react *in vitro* with linoleoyl-CoA. Using the butylamidation method, acyl-CoA substrate and product were detected by gas chromatography specifically. In my knowledge, this is the first study to detect the *in vitro* desaturation product using non-labeled acyl-CoA as the substrate.

In chapter 4, I constructed the purification system of cytochrome b_5 fusion protein including D6d and D5d for crystal structure analysis. Active D6d and D5d were successfully expressed in the methylotrophic yeast, *Pichia pastoris*, and I conducted the large-scale desaturase production system using a jar fermenter. D6d and D5d were solubilized with *n*-dodecyl-ß-maltoside, *n*-decyl-ß-maltoside and Triton X-100 efficiently. Each desaturase was

purified to homogeneity using an affinity chromatography and a gel filtration chromatography.

Taken together, I got the important knowledge that contributes to furthering our understanding about the structure-function relationship of desaturase family. Since these enzymes have a high structural similarity, it is estimated that other related enzymes have also mechanism similar to the substrate specificity determining mechanism of D6d and D5d (Chapter 1). Therefore, this information can be the key to exhaustive elucidation of the molecular mechanism of various reaction specificities of desaturase family. In addition, a structural biology approach (Chapter 4) can clarify the target to produce enzymes with desired functions by unraveling of enzyme-substrate interactions. Simpler *in vitro* reaction method of acyl-CoA desaturase (chapter 3) enables precise characterization of artificial enzymes. This knowledge will enable us to produce enzymes performing the specific modifications to any portion of the hydrocarbon chains, and these enzymes will be useful to the design of high value-added fatty acids.

Elucidation of crystal structure of human stearoyl-CoA desaturase (22, 23) encouraged the dramatic progress in the understandings of the structure-function relationship of these enzymes. Combined the structural information with reports accumulated previously, the whole picture of the reaction mechanisms of desaturase family enzymes will be revealed completely in the near future. I hope the further progress of this research and believe that the results obtained in my study become important foundations.

Acknowledgements

I would have never been able to finish this thesis without the encouragement and help of many individuals. First and foremost, I would like to express the deepest appreciation to my supervisor, Professor Tsunehiro Aki, for his excellent guidance, patience and immense knowledge throughout my study.

I would also like to thank Professor Nobukazu Tanaka and Professor Seiji Kawamoto, for carefully reviewing this work. I would also thank to Professor Junichi Kato, for kindly reviewing in my research of master course.

I appreciate Associate Professor Kenji Arakawa and Associate Professor Yoshiko Okamura for their technical guidance and encouragement. I thank Dr. Tomoko Amimoto for her kind support with MS analyses.

I would like to thank for all the members of the laboratory of Cell Biochemistry for their kindness and friendship.

Finally, I have a deep appreciation for the financial support of all our group members of Core Research for Evolutional Science and Technology (CREST) and Japan Science and Technology Agency (JST).

References

1. Smith, S., Witkowski, A., and Joshi, A. K. (2003) Structural and functional organization of the animal fatty acid synthase. *Prog. Lipid Res.* **42**, 289–317
2. Tapiero, H., Nguyen Ba, G., Couvreur, P., and Tew, K. D. (2002) Polyunsaturated fatty acids (PUFA) and eicosanoids in human health and pathologies. *Biomed. Pharmacother.* **56**, 215–222
3. Carlson, S. E. (2001) Docosahexaenoic acid and arachidonic acid in infant development. *Semin. Neonatol.* **6**, 437–449
4. Koletzko, B., Lien, E., Agostoni, C., Böhles, H., Campoy, C., Cetin, I., Decsi, T., Dudenhausen, J. W., Dupont, C., Forsyth, S., Hoesli, I., Holzgreve, W., Lapillonne, A., Putet, G., Secher, N. J., Symonds, M., Szajewska, H., Willatts, P., and Uauy, R. (2008) The roles of long-chain polyunsaturated fatty acids in pregnancy, lactation and infancy: Review of current knowledge and consensus recommendations. *J. Perinat. Med.* **36**, 5–14
5. Luo, T., Sakai, Y., Wagner, E., and Drager, U. C. (2006) Retinoids, eye development, and maturation of visual function. *J. Neurobiol.* **66**, 677–686
6. Kinsella, J. E., Broughton, K. S., and Whelan, J. W. (1990) Dietary unsaturated fatty acids: Interactions and possible needs in relation to eicosanoid synthesis. *J. Nutr. Biochem.* **1**, 123–141
7. Natarajan, R. (2004) Lipid Inflammatory Mediators in Diabetic Vascular Disease. *Arterioscler. Thromb. Vasc. Biol.* **24**, 1542–1548
8. Chen, X., Goodwin, S. M., Boroff, V. L., Liu, X., and Jenks, M. A. (2003) Cloning and characterization of the WAX2 gene of Arabidopsis involved in cuticle membrane and wax production. *Plant Cell*. **15**, 1170–1185
9. Pohl, C. H., Kock, J. L. F., and Thibane, V. S. (2011) Antifungal free fatty acids: a

review. *Sci. against Microb. Pathog. Curr. Res. Technol. Adv.* **1**, 61–71

10. Blée, E., Flenet, M., Boachon, B., and Fauconnier, M. L. (2012) A non-canonical caleosin from *Arabidopsis* efficiently epoxidizes physiological unsaturated fatty acids with complete stereoselectivity. *FEBS J.* **279**, 3981–3995
11. Hargrave, K. M., Meyer, B. J., Li, C., Azain, M. J., Baile, C. A., and Miner, J. L. (2004) Influence of dietary conjugated linoleic acid and fat source on body fat and apoptosis in mice. *Obes. Res.* **12**, 1435–1444
12. Shanklin, J., and Somerville, C. (1991) Stearoyl-acyl-carrier-protein desaturase from higher plants is structurally unrelated to the animal and fungal homologs. *Proc. Natl. Acad. Sci. U. S. A.* **88**, 2510–2514
13. Aki, T., Shimada, Y., Inagaki, K., Higashimoto, H., Kawamoto, S., Shigeta, S., Ono, K., and Suzuki, O. (1999) Molecular cloning and functional characterization of rat Δ6 fatty acid desaturase. *Biochem. Biophys. Res. Commun.* **255**, 575–579
14. Sakuradani, E., Kobayashi, M., and Shimizu, S. (1999) Δ6-Fatty acid desaturase from an arachidonic acid-producing *Mortierella* fungus: Gene cloning and its heterologous expression in a fungus, Aspergillus. *Gene*. **238**, 445–453
15. Michaelson, L. V, Zäuner, S., Markham, J. E., Haslam, R. P., Desikan, R., Mugford, S., Albrecht, S., Warnecke, D., Sperling, P., Heinz, E., and Napier, J. A. (2009) Functional characterization of a higher plant sphingolipid Δ4-desaturase: defining the role of sphingosine and sphingosine-1-phosphate in Arabidopsis. *Plant Physiol.* **149**, 487–498
16. Passorn, S., Laoteng, K., Rachadawong, S., Tanticharoen, M., and Cheevadhanarak, S. (1999) Heterologous expression of *Mucor rouxii* Δ12-desaturase gene in *Saccharomyces cerevisiae*. *Biochem. Biophys. Res. Commun.* **263**, 47–51
17. Shanklin, J., Whittle, E., and Fox, B. G. (1994) Eight histidine residues are catalytically essential in a membrane-associated iron enzyme, stearoyl-CoA desaturase, and are conserved in alkane hydroxylase and xylene monooxygenase. *Biochemistry*. **33**, 12787–

12794

18. Lindqvist, Y., Huang, W., Schneider, G., and Shanklin, J. (1996) Crystal structure of Δ9 stearoyl-acyl carrier protein desaturase from castor seed and its relationship to other di-iron proteins. *EMBO J.* **15**, 4081–4092

19. Li, S. F., Song, L. Y., Zhang, G. J., Yin, W. B., Chen, Y. H., Wang, R. R. C., and Hu, Z. M. (2011) Newly identified essential amino acid residues affecting Δ8-sphingolipid desaturase activity revealed by site-directed mutagenesis. *Biochem. Biophys. Res. Commun.* **416**, 165–171

20. Song, L. Y., Lu, W. X., Hu, J., Yin, W. B., Chen, Y. H., Wang, B. L., Wang, R. R. C., and Hu, Z. M. (2013) The role of C-terminal amino acid residues of a Δ^6-fatty acid desaturase from blackcurrant. *Biochem. Biophys. Res. Commun.* **431**, 675–679

21. Sayanova, O., Beaudoin, F., Libisch, B., Castel, A., Shewry, P. R., and Napier, J. A. (2001) Mutagenesis and heterologous expression in yeast of a plant Δ6-fatty acid desaturase. *J. Exp. Bot.* **52**, 1581–1585

22. Wang, H., Klein, M. G., Zou, H., Lane, W., Snell, G., Levin, I., Li, K., and Sang, B. C. (2015) Crystal structure of human stearoyl–coenzyme A desaturase in complex with substrate. *Nat. Struct. Mol. Biol.* **22**, 581–585

23. Bai, Y., McCoy, J. G., Levin, E. J., Sobrado, P., Rajashankar, K. R., Fox, B. G., and Zhou, M. (2015) X-ray structure of a mammalian stearoyl-CoA desaturase. *Nature*. **524**, 252–256

24. Brejc, K., van Dijk, W. J., Klaassen, R. V, Schuurmans, M., van Der Oost, J., Smit, A. B., and Sixma, T. K. (2001) Crystal structure of an ACh-binding protein reveals the ligand-binding domain of nicotinic receptors. *Nature*. **411**, 269–276

25. Russell, R. J., Haire, L. F., Stevens, D. J., Collins, P. J., Lin, Y. P., Blackburn, G. M., Hay, A. J., Gamblin, S. J., and Skehel, J. J. (2006) The structure of H5N1 avian influenza neuraminidase suggests new opportunities for drug design. *Nature*. **443**, 45–49

26. Xu, X. (2000) Production of specific-structured triacylglycerols by lipase-catalyzed reactions: a review. *Eur. J. Lipid Sci. Technol.* **102**, 287–303

27. Cho, H. P., Nakamura, M., and Clarke, S. D. (1999) Cloning, expression, and fatty acid regulation of the human Δ5 desaturase. *J. Biol. Chem.* **274**, 37335–37339

28. Michinaka, Y., Aki, T., Inagaki, K., Higashimoto, H., Shimada, Y., Nakajima, T., Shimauchi, T., Ono, K., and Suzuki, O. (2001) Production of polyunsaturated fatty acids by genetic engineering of yeast. *J. Oleo Sci.* **50**, 359–365

29. McKeon, T. A., and Stumpf, P. K. (1982) Purification and characterization of the stearoyl-acyl carrier protein desaturase and the acyl-acyl carrier protein thioesterase from maturing seeds of safflower. *J. Biol. Chem.* **257**, 12141–12147

30. Watts, J. L., and Browse, J. (1999) Isolation and characterization of a Δ5-fatty acid desaturase from *Caenorhabditis elegans*. *Arch. Biochem. Biophys.* **362**, 175–182

31. Knutzon, D. S., Thurmond, J. M., Huang, Y. S., Chaudhary, S., Bobik, E. G., Chan, G. M., Kirchner, S. J., and Mukerji, P. (1998) Identification of Δ5-desaturase from *Mortierella alpina* by heterologous expression in bakers' yeast and canola. *J. Biol. Chem.* **273**, 29360–29366

32. Guy, J. E., Whittle, E., Moche, M., Lengqvist, J., Lindqvist, Y., and Shanklin, J. (2011) Remote control of regioselectivity in acyl-acyl carrier protein-desaturases. *Proc. Natl. Acad. Sci.* **108**, 16594–16599

33. Sayanova, O., Shewry, P. R., and Napier, J. A. (1999) Histidine-41 of the cytochrome b_5 domain of the borage Δ^6 fatty acid desaturase is essential for enzyme activity. *Plant Physiol.* **121**, 641–646

34. Gostinčar, C., Turk, M., and Gunde-Cimerman, N. (2010) The evolution of fatty acid desaturases and cytochrome *b5* in eukaryotes. *J. Membr. Biol.* **233**, 63–72

35. Guillou, H., Rioux, V., Catheline, D., Thibault, J.-N., Bouriel, M., Jan, S., D'Andrea, S., and Legrand, P. (2003) Conversion of hexadecanoic acid to hexadecenoic acid by rat Δ

6-desaturase. *J. Lipid Res.* **44**, 450–454

36. Meesapyodsuk, D., and Qiu, X. (2012) The front-end desaturase: Structure, function, evolution and biotechnological use. *Lipids*. **47**, 227–237

37. Sasata, R. J., Reed, D. W., Loewen, M. C., and Covello, P. S. (2004) Domain swapping localizes the structural determinants of regioselectivity in membrane-bound fatty acid desaturases of *Caenorhabditis elegans*. *J. Biol. Chem.* **279**, 39296–39302

38. Hoffmann, M., Hornung, E., Busch, S., Kassner, N., Ternes, P., Braus, G. H., and Feussner, I. (2007) A small membrane-peripheral region close to the active center determines regioselectivity of membrane-bound fatty acid desaturases from *Aspergillus nidulans*. *J. Biol. Chem.* **282**, 26666–26674

39. Song, L. Y., Zhang, Y., Li, S. F., Hu, J., Yin, W. B., Chen, Y. H., Hao, S. T., Wang, B. L., Wang, R. R. C., and Hu, Z. M. (2014) Identification of the substrate recognition region in the Δ6-fatty acid and Δ8-sphingolipid desaturase by fusion mutagenesis. *Planta*. **239**, 753–763

40. Na-Ranong, S., Laoteng, K., Kittakoop, P., Tanticharoen, M., and Cheevadhanarak, S. (2006) Targeted mutagenesis of a fatty acid Δ6-desaturase from *Mucor rouxii*: Role of amino acid residues adjacent to histidine-rich motif II. *Biochem. Biophys. Res. Commun.* **339**, 1029–1034

41. Lim, Z. L., Senger, T., and Vrinten, P. (2014) Four amino acid residues influence the substrate chain-length and regioselectivity of Siganus canaliculatus Δ4 and Δ5/6 desaturases. *Lipids*. **49**, 357–367

42. Meesapyodsuk, D., and Qiu, X. (2014) Structure determinants for the substrate specificity of acyl-CoA Δ9 desaturases from a marine copepod. *ACS Chem. Biol.* **9**, 922–934

43. Vanhercke, T., Shrestha, P., Green, A. G., and Singh, S. P. (2011) Mechanistic and structural insights into the regioselectivity of an acyl-CoA fatty acid desaturase via

directed molecular evolution. *J. Biol. Chem.* **286**, 12860–12869

44. Broun, P., Boddupalli, S., and Somerville, C. (1998) A bifunctional oleate 12-hydroxylase: desaturase from *Lesquerella fendleri*. *Plant J.* **13**, 201–210

45. Gagné, S. J., Reed, D. W., Gray, G. R., and Covello, P. S. (2009) Structural control of chemoselectivity, stereoselectivity, and substrate specificity in membrane-bound fatty acid acetylenases and desaturases. *Biochemistry*. **48**, 12298–12304

46. Rawat, R., Yu, X. H., Sweet, M., and Shanklin, J. (2012) Conjugated fatty acidsynthesis. residues 111 and 115 influence product partitioning of *Momordica charantia* conjugase. *J. Biol. Chem.* **287**, 16230–16237

47. Hastings, N., Agaba, M., Tocher, D. R., Leaver, M. J., Dick, J. R., Sargent, J. R., and Teale, A. J. (2001) A vertebrate fatty acid desaturase with Δ5 and Δ6 activities. *Proc. Natl. Acad. Sci. U. S. A.* **98**, 14304–14309

48. Wang, H., Klein, M. G., Zou, H., Lane, W., Snell, G., Levin, I., Li, K., and Sang, B. C. (2015) Crystal structure of human stearoyl–coenzyme A desaturase in complex with substrate. *Nat. Struct. Mol. Biol.* **22**, 581–585

49. Ito, H., Fukuda, Y., and Murata, K. (1983) Transformation of intact yeast cells treated with alkali cations. *J. Bacteriol.* **153**, 166–168

50. Laemmli, U. K. (1970) Cleavage of structural proteins during the assembly of the head of bacteriophage T4. *Nature*. **227**, 680–685

51. Cho, H. P., Nakamura, M. T., and Clarke, S. D. (1999) Cloning, expression, and nutritional regulation of the mammalian Δ6 desaturase. *J. Biol. Chem.* **274**, 471–477

52. International Chicken Genome Sequencing Consortium (2004) Sequence and comparative analysis of the chicken genome provide unique perspectives on vertebrate evolution. *Nature*. **432**, 695–716

53. Zheng, X., Tocher, D. R., Dickson, C. A., Bell, J. G., and Teale, A. J. (2005) Highly unsaturated fatty acid synthesis in vertebrates: new insights with the cloning and

characterization of a Δ6 desaturase of Atlantic salmon. *Lipids*. **40**, 13–24

54. Hastings, N., Agaba, M. K., Tocher, D. R., Zheng, X., Dickson, C. a., Dick, J. R., and Teale, A. J. (2004) Molecular cloning and functional characterization of fatty acyl desaturase and elongase cDNAs involved in the production of eicosapentaenoic and docosahexaenoic acids from α-linolenic acid in Atlantic salmon (*Salmo salar*). *Mar. Biotechnol.* **6**, 463–474

55. Castro, L. F. C., Monroig, Ó., Leaver, M. J., Wilson, J., Cunha, I., and Tocher, D. R. (2012) Functional desaturase Fads1 (Δ5) and Fads2 (Δ6) orthologues evolved before the origin of jawed vertebrates. *PLoS One*. **7**, 1–9

56. Li, Y. Y., Hu, C. B., Zheng, Y. J., Xia, X. A., Xu, W. J., Wang, S. Q., Chen, W. Z., Sun, Z. W., and Huang, J. H. (2008) The effects of dietary fatty acids on liver fatty acid composition and Δ6-desaturase expression differ with ambient salinities in *Siganus canaliculatus*. *Comp. Biochem. Physiol. B. Biochem. Mol. Biol.* **151**, 183–190

57. Kelley, L. A., Mezulis, S., Yates, C. M., Wass, M. N., and Sternberg, M. J. E. (2015) The Phyre2 web portal for protein modeling , prediction and analysis. *Nat. Protoc.* **10**, 845–858

58. Eckhardt, M., Yaghootfam, A., Fewou, S. N., Zöller, I., and Gieselmann, V. (2005) A mammalian fatty acid hydroxylase responsible for the formation of alpha-hydroxylated galactosylceramide in myelin. *Biochem. J.* **388**, 245–254

59. Dyer, J. M., Chapital, D. C., Kuan, J. W., Mullen, R. T., Turner, C., Mckeon, T. A., and Pepperman, A. B. (2002) Molecular analysis of a bifunctional fatty acid conjugase/desaturase from tung. Implications for the evolution of plant fatty acid diversity. *Plant Physiol.* **130**, 2027–2038

60. Sperling, P., Lee, M., Girke, T., Za, U., Stymne, S., and Heinz, E. (2000) A bifunctional Δ6−fatty acyl acetylenase/desaturase from the moss *Ceratodon purpureus*. *Plant Breed.* **267**, 3801–3811

61. Hamberg, M., and Fahlstadius, P. (1992) On the specificity of a fatty acid epoxygenase in broad bean (*Vicia faba* L.). *Plant Physiol.* **99**, 987–995

62. Hong, H., Datla, N., MacKenzie, S. L., and Qiu, X. (2002) Isolation and characterization of a Δ5 FA desaturase from *Pythium irregulare* by heterologous expression in *Saccharomyces cerevisiae* and oilseed crops. *Lipids*. **37**, 863–868

63. Wallis, J. G., Watts, J. L., and Browse, J. (2002) Polyunsaturated fatty acid synthesis: What will they think of next? *Trends Biochem. Sci.* **27**, 467–473

64. Sayanova, O., Smith, M. A., Lapinskas, P., Stobart, A. K., Dobson, G., Christie, W. W., Shewry, P. R., and Napier, J. A. (1997) Expression of a borage desaturase cDNA containing an N-terminal cytochrome *b*5 domain results in the accumulation of high levels of Δ6-desaturated fatty acids in transgenic tobacco. *Proc. Natl. Acad. Sci. U. S. A.* **94**, 4211–4216

65. Brenner, R. R., and Peluffo, R. O. (1966) Effect of saturated and unsaturated fatty acids on the desaturation *in vitro* of palmitic, stearic, oleic, linoleic, and linolenic acids. *J. Biol. Chem.* **241**, 5213–5219

66. Norman, H. A., Pillai, P., and St. John, J. B. (1991) *In vitro* desaturation of monogalactosyldiacylglycerol and phosphatidylcholine molecular species by chloroplast homogenates. *Phytochemistry*. **30**, 2217–2222

67. Girke, T., Schmidt, H., Zähringer, U., Reski, R., and Heinz, E. (1998) Identification of a novel Δ 6-acyl-group desaturase by targeted gene disruption in *Physcomitrella patens*. *Plant J.* **15**, 39–48

68. Zank, T. K., Zähringer, U., Beckmann, C., Pohnert, G., Boland, W., Holtorf, H., Reski, R., Lerchl, J., and Heinz, E. (2002) Cloning and functional characterisation of an enzyme involved in the elongation of Δ6-polyunsaturated fatty acids from the moss *Physcomitrella patens*. *Plant J.* **31**, 255–268

69. Schultz, D. J., Cahoon, E. B., Shanklin, J., Craig, R., Cox-Foster, D. L., Mumma, R. O.,

and Medford, J. I. (1996) Expression of a Δ9 14:0-acyl carrier protein fatty acid desaturase gene is necessary for the production of ω5 anacardic acids found in pest-resistant geranium (*Pelargonium xhortorum*). *Proc. Natl. Acad. Sci. U. S. A.* **93**, 8771–8775

70. Sakuradani, E., Kobayashi, M., Ashikari, T., and Shimizu, S. (1999) Identification of Δ12-fatty acid desaturase from arachidonic acid-producing *Mortierella* fungus by heterologous expression in the yeast *Saccharomyces cerevisiae* and the fungus *Aspergillus oryzae*. *Eur. J. Biochem.* **261**, 812–820

71. Spychalla, J. P., Kinney, A. J., and Browse, J. (1997) Identification of an animal omega-3 fatty acid desaturase by heterologous expression in *Arabidopsis*. *Proc. Natl. Acad. Sci. U. S. A.* **94**, 1142–1147

72. Stukey, J. E., McDonough, V. M., and Martin, C. E. (1990) The OLE1 gene of Saccharomyces cerevisiae encodes the Δ9 fatty acid desaturase and can be functionally replaced by the rat stearoyl-CoA desaturase gene. *J. Biol. Chem.* **265**, 20144–20149

73. Sayanova, O., Haslam, R., Guschina, I., Lloyd, D., Christie, W. W., Harwood, J. L., and Napier, J. A. (2006) A bifunctional Δ12, Δ15-desaturase from *Acanthamoeba castellanii* directs the synthesis of highly unusual n-1 series unsaturated fatty acids. *J. Biol. Chem.* **281**, 36533–36541

74. Haritos, V. S., Horne, I., Damcevski, K., Glover, K., and Gibb, N. (2014) Unexpected functional diversity in the fatty acid desaturases of the flour beetle *Tribolium castaneum* and identification of key residues determining activity. *Insect Biochem. Mol. Biol.* **51**, 62–70

75. Smith, P. K., Krohn, R. I., Hermanson, G. T., Mallia, A. K., Gartner, F. H., Provenzano, M. D., Fujimoto, E. K., Goeke, N. M., Olson, B. J., and Klenk, D. C. (1985) Measurement of protein using bicinchoninic acid. *Anal. Biochem.* **150**, 76–85

76. Kopka, J., Ohlrogge, J. B., and Jaworski, J. G. (1995) Analysis of *in vivo* levels of

acyl-thioesters with gas chromatography/mass spectrometry of the butylamide derivative. *Anal. Biochem.* **224**, 51–60

77. Kawaguchi, A., Yoshimura, T., and Okuda, S. (1981) A new method for the preparation of acyl-CoA thioesters. *J. Biol. Chem.* **89**, 337–339

78. Guillou, H., D'Andrea, S., Rioux, V., Barnouin, R., Dalaine, S., Pedrono, F., Jan, S., and Legrand, P. (2004) Distinct roles of endoplasmic reticulum cytochrome b5 and fused cytochrome b5-like domain for rat Δ6-desaturase activity. *J. Lipid Res.* **45**, 32–40

79. Jeffcoat, R., Dunton, A. P., and James, A. T. (1978) Evidence for the different responses of Δ^9-, Δ^6- and Δ^5-fatty acyl-CoA desaturases to cytoplasmic proteins. *Biochim. Biophys. Acta*. **528**, 28–35

80. Browse, J. A., and Slack, C. R. (1981) Catalase stimulates linoleate desaturase activity in microsomes from developing linseed cotyledons. *FEBS Lett.* **131**, 111–114

81. Shanklin, J., Guy, J. E., Mishra, G., and Lindqvist, Y. (2009) Desaturases: Emerging models for understanding functional diversification of diiron-containing enzymes. *J. Biol. Chem.* **284**, 18559–18563

82. Oshino, N., Imai, Y., and Sato, R. (1971) A function of cytochrome b5 in fatty acid desaturation by rat liver microsomes. *J. Biochem.* **69**, 155–167

83. Folch, J., Lees, M., and Stanley, G. H. S. (1957) A simple method for the isolation and purification of total lipids from animal tissues. *J Biol Chem*. **226**, 497–509

84. Wu, S., and Letchworth, G. J. (2004) High efficiency transformation by electroporation of *Pichia pastoris* pretreated with lithium acetate and dithiothreitol. *Biotechniques*. **36**, 152–154

85. Goren, M. A., and Fox, B. G. (2008) Wheat germ cell-free translation, purification, and assembly of a functional human stearoyl-CoA desaturase complex. *Protein Expr Purif.* **62**, 171–178

86. Chen, H., Gu, Z., Zhang, H., Wang, M., Chen, W., Lowther, W. T., and Chen, Y. Q.

(2013) Expression and purification of integral membrane fatty acid desaturases. *PLoS One*. **8**, 1–9

87. Koronakis, V., Sharff, A., Koronakis, E., Luisi, B., and Hughes, C. (2000) Crystal structure of the bacterial membrane protein TolC central to multidrug efflux and protein export. *Nature*. **405**, 914–919

88. Cherezov, V., Rosenbaum, D. M., Hanson, M. A., Rasmussen, S. G. F., Thian, F. S., Kobilka, T. S., Choi, H. J., Kuhn, P., Weis, W. I., Kobilka, B. K., and Stevens, R. C. (2008) High resolution crystal structure of an engineered human β2 adrenergic G protein coupled receptor. *Science.* **318**, 1258–1265

89. Murakami, S., Nakashima, R., Yamashita, E., and Yamaguchi, A. (2002) Crystal structure of bacterial multidrug efflux transporter AcrB. *Nature*. **419**, 587–593

90. Tsukazaki, T., Mori, H., Fukai, S., Numata, T., Perederina, A., Adachi, H., Matsumura, H., Takano, K., Murakami, S., Inoue, T., Mori, Y., Sasaki, T., Vassylyev, D. G., Nureki, O., and Ito, K. (2006) Purification, crystallization and preliminary X-ray diffraction of SecDF, a translocon-associated membrane protein, from *Thermus thermophilus*. *Acta Crystallogr. Sect. F Struct. Biol. Cryst. Commun.* **62**, 376–380

91. Watanabe, K., Ohno, M., and Aki, T. (2016) Detection of acyl-CoA derivatized with butylamide for *in vitro* fatty acid desaturase assay. *J. Oleo Sci.* **65**, 161–167

92. Yoshida, Y., and Kumaoka, H. (1975) Studies on the microsomal electron-transport system of anaerobically grown yeast: III. spectral characterization of cytochrome P-450. *J. Biochem.* **78**, 785–794

公表論文

（1）Identification of amino acid residues that determine the substrate specificity of mammalian membrane-bound front-end fatty acid desaturases

K. Watanabe, M. Ohno, M. Taguchi, S. Kawamoto, K. Ono, T. Aki

Journal of Lipid Research, **57**, 89-99 (2016)

（2）Detection of acyl-CoA derivatized with butylamide for *in vitro* fatty acid desaturase assay

K. Watanabe, M. Ohno, T. Aki

Journal of Oleo Science, **65**, 161-167 (2016)